# CHAPTER 6

# RESULTS AND DISCUSSIONS

The numerical and experimental results for film cooling effectiveness for all studied cases are presented in this chapter. The results obtained from the baseline case geometry are used as a reference for all other cases. A comparison between numerical and experimental is presented in this chapter to show the verification of the numerical model. Comparison between the present work and some of previous work, which treated with the anti-vortex technique or has the same baseline as compared with the present work, are also presented at the end of this chapter.

## 6.1 Numerical Results

The detailed numerical results film cooling effectiveness for all points in the domain is presented in this section. The experimental results film cooling effectiveness is available at the measured stations only at which thermocouples are used to measure the test surface temperature. The velocity vectors which present the interaction between the mainstream flow and the coolant jet flow will be presented in details in the discussion part.

### 6.1.1 Film Cooling Effectiveness

Figure (6.1), (6.2), (6.3), (6.4) show the effect of velocity ratio on detailed film cooling effectiveness distributions for all four cases with zero pressure gradient (ZPG) and applied pressure gradient (APG(1)). The shown data in figures were taken at the test surface downstream the film holes (at y = 0).

For baseline, figure (6.1) shows that the highest film cooling effectiveness occurring with the lowest velocity ratio (VR = 0.5) for both ZPG and APG(1). As the velocity ratio increases, the momentum ratio increases causing the jet to penetrate the mainstream flow and lift-off away from the test surface. So the film cooling effectiveness decreases as the velocity ratio increases.

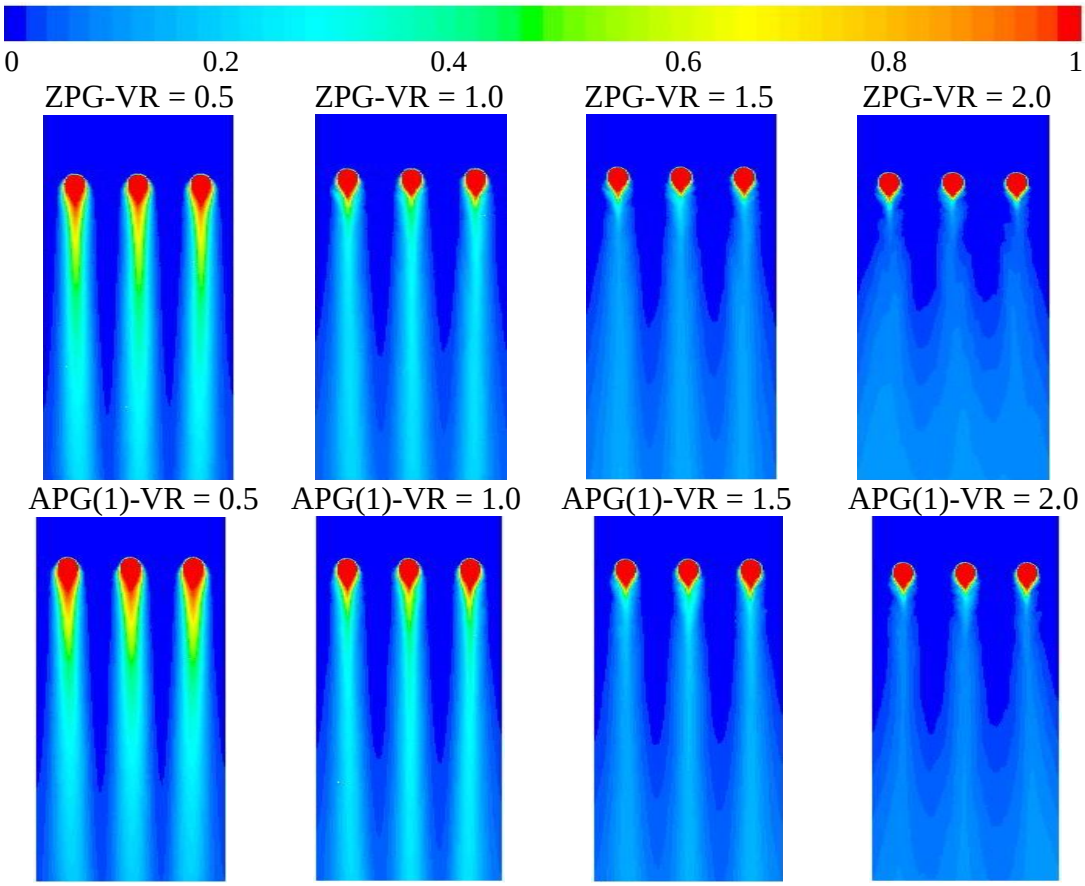


Figure (6.1) Detailed Film Cooling Effectiveness Distributions for Baseline Case under ZPG and APG(1) at different Velocity ratios

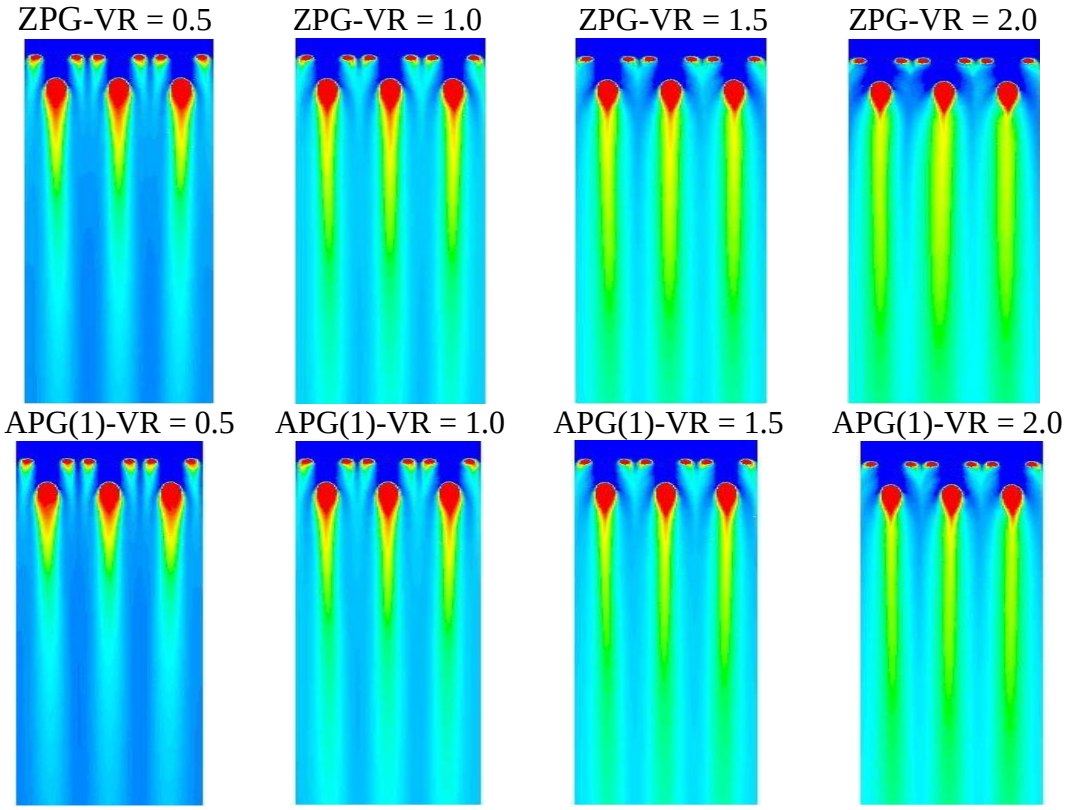


Figure (6.2) Detailed Film Cooling Effectiveness Distributions for Case-1 under ZPG and APG(1) at different Velocity ratios

For case 1, the anti vortex holes are half the size of the main hole and exit upstream of the main hole. Figure (6.2) shows that the film cooling effectiveness is higher than baseline case for all velocity ratios but the trend is different from baseline, as the velocity ratio increases the film cooling effectiveness increases and covers bigger area. The anti-vortex pair cause reduced flow through the main hole and also supplements the overall coverage in the region between the holes. The highest effectiveness occurs at velocity ratio of 2.0. The effect of this anti-vortex pair appears to mainly reduce the coolant momentum flux from the main holes. The effect of APG(1) appears slightly different from ZPG but the covered area, downstream the coolant jet, appears thinner and shorter with APG(1) than ZPG especially with higher velocity ratio.

For case 2, as shown in figure (6.3), the anti vortex holes are also half the size of the main hole and still exit upstream of the main hole but more close to the main hole than in case 1. Like in case 1, the film effectiveness increases as the velocity ratio increases. But the film cooling effectiveness downstream the anti vortex holes decreases as the velocity ratio increases. So the regions between holes have less effectiveness than that in case 1. As the pressure is applied for all velocity ratios, the film effectiveness has small change especially in the regions between holes.

In case 3, as shown in figure (6.4) the anti vortex holes are also half the size of the main hole but exit in the same line with the main hole. The trend of the film effectiveness is return to be similar to that of the baseline just downstream the main hole, as the velocity ratio increases, the film effectiveness decreases. But the film effectiveness is still higher than that of the baseline. Figure (6.4) shows that the film cooling effectiveness covered area gets narrower as the flow moves downstream the film holes. The flow from anti-vortex holes moves under the flow from the main holes causing the main hole jet to lift off from the surface especially with higher velocity ratios. The effect of APG(1) is slightly different from ZPG. More details about the APG(1) effect will appear in spanwise averaged film cooling effectiveness.

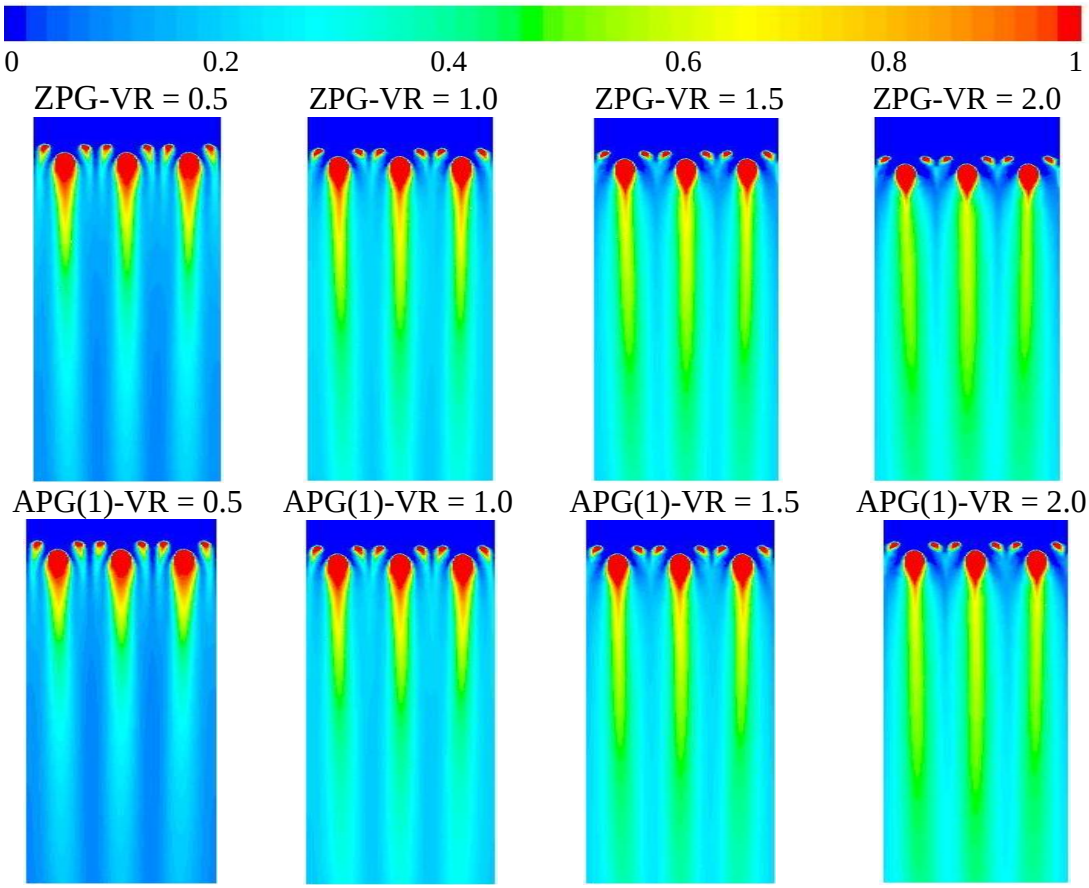


Figure (6.3) Detailed Film Cooling Effectiveness Distributions for Case-2 under ZPG and APG(1) at different Velocity ratios

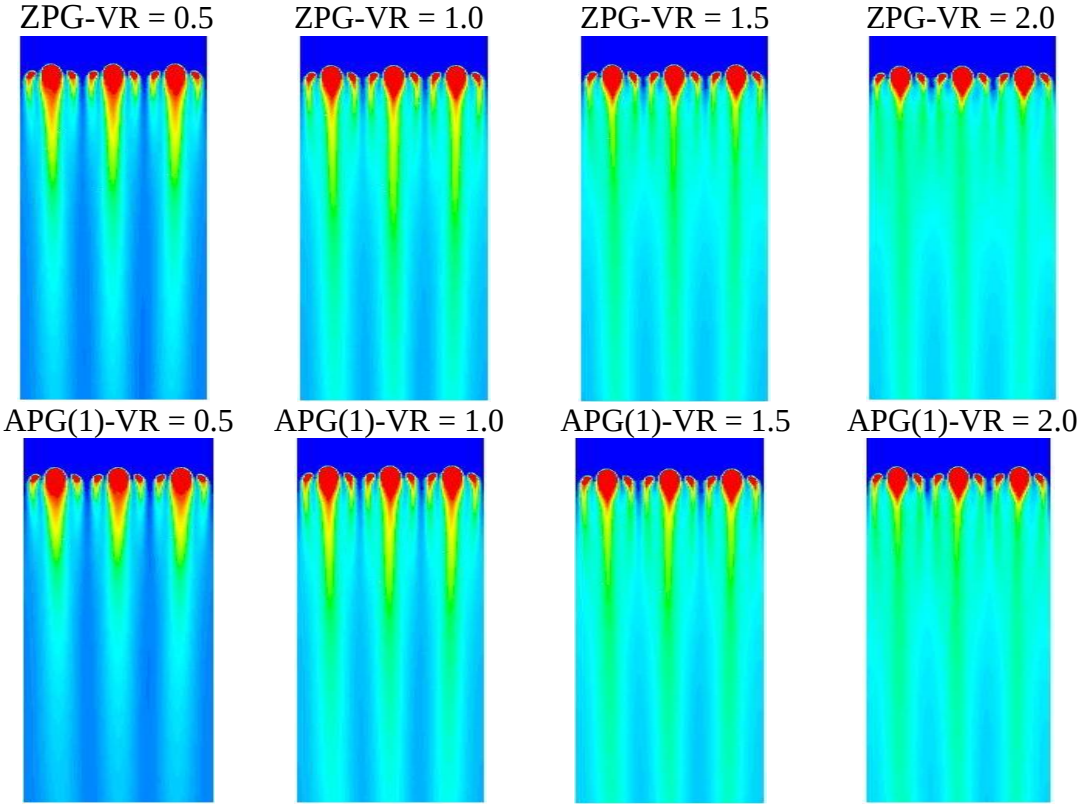


Figure (6.4) Detailed Film Cooling Effectiveness Distributions for Case-3 under ZPG and APG(1) at different Velocity ratios

### 6.1.2 Spanwise Averaged Film Cooling Effectiveness

The spanwise averaged was calculated for points from z/D = 1.5 to z/D = -1.5, it means that the spanwise averaged film cooling effectiveness will be presented downstream the middle hole. Figures (6.5), (6.6), (6.7), and (6.8) shows the spanwise averaged film cooling effectiveness for all cases with ZPG and APG(1) at VR = 0.5, 1.0, 1.5, and 2.0 respectively.

For VR = 0.5, Figure (6.5) shows that, for all cases under ZPG or APG(1), the spanwise film cooling effectiveness decreases as x/D increases. The momentum ratio at VR = 0.5 is low and accordingly the jet flow doesn't penetrate the main stream flow. It moves below the main stream flow and the film cooling effectiveness continuous to decrease with x/D for all cases. The anti-vortex cases give a higher film cooling effectiveness as compared with baseline case. The film cooling effectiveness with anti-vortex cases appears close to each other. Such improvement in film cooling effectiveness can be explained by the close contact between the cooling fluid and the surface. The stream lines produced by FLUENT shows a wider cooling area for all anti-vortex cases as compared with the baseline case. Case 3 gives the highest film cooling effectiveness along the studied spanwise under ZPG or APG(1). In case 3 the flow out from the anti-vortex holes is inline with the flow from the main holes and both of them is moving beside the test surface which gives a wider cooling area as compared with other cases.

For VR = 1.0, Figure (6.6) shows that, for baseline under ZPG, the film cooling effectiveness starts from high value near the hole exit and begins to decrease rapidly until x/D = 7 then the film effectiveness begins to increase slowly. For APG(1) baseline, the film effectiveness takes the same trend as ZPG baseline but with higher values. The anti-vortex cases still have the same trend as compared with the same cases at VR =0.5 but with higher values. Under ZPG, the highest film effectiveness is given by case 3 near the holes exit until x/D =9 after which the highest film effectiveness is given by case 2. Case 1 gives the same film effectiveness as case 2 near the hole exit until x/D = 5 then it gives lower effectiveness. The spanwise film effectiveness for APG(1) is lower than that with ZPG for case 1 and case 2.

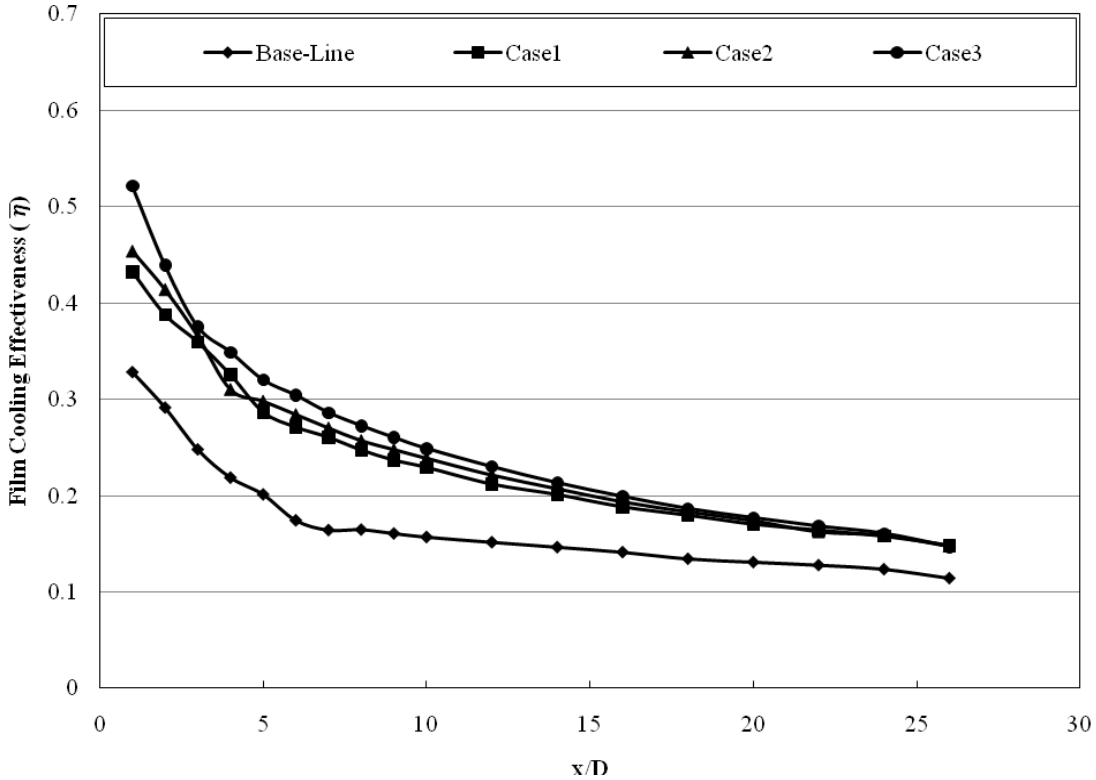


a) Under ZPG

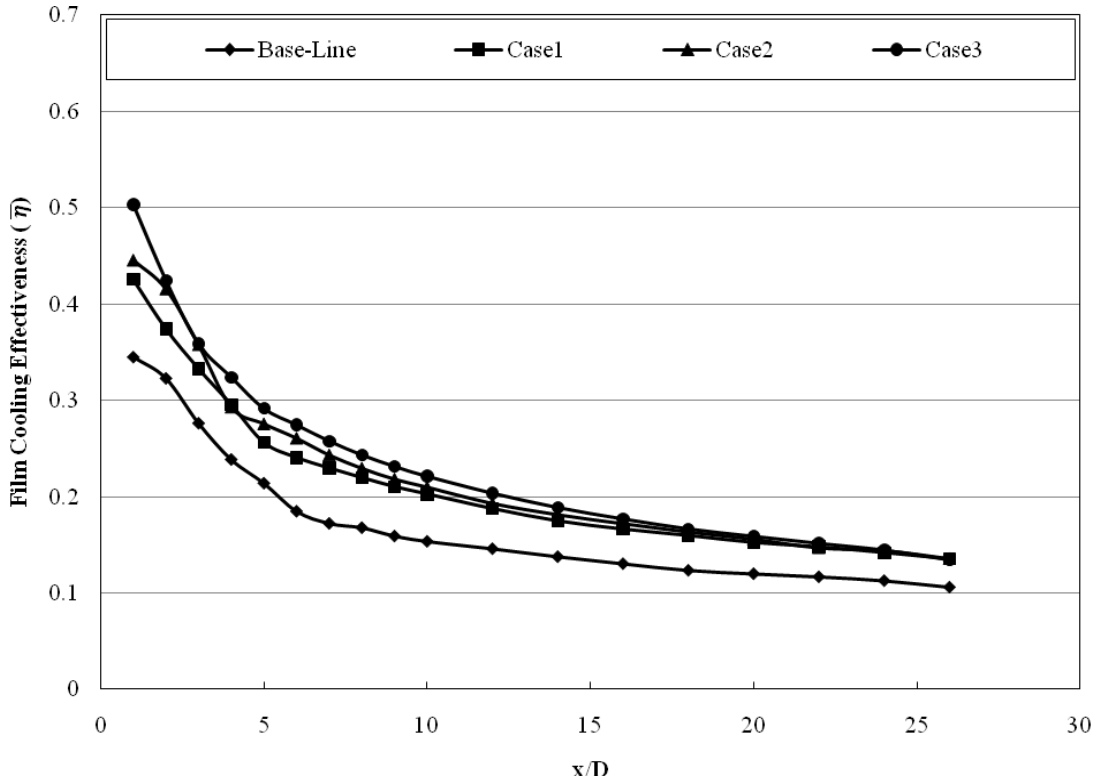


b) Under APG(1)

Figure (6.5) Spanwise Averaged Film Cooling Effectiveness Distributions under ZPG and APG(1) at VR = 0.5 (Numerical)

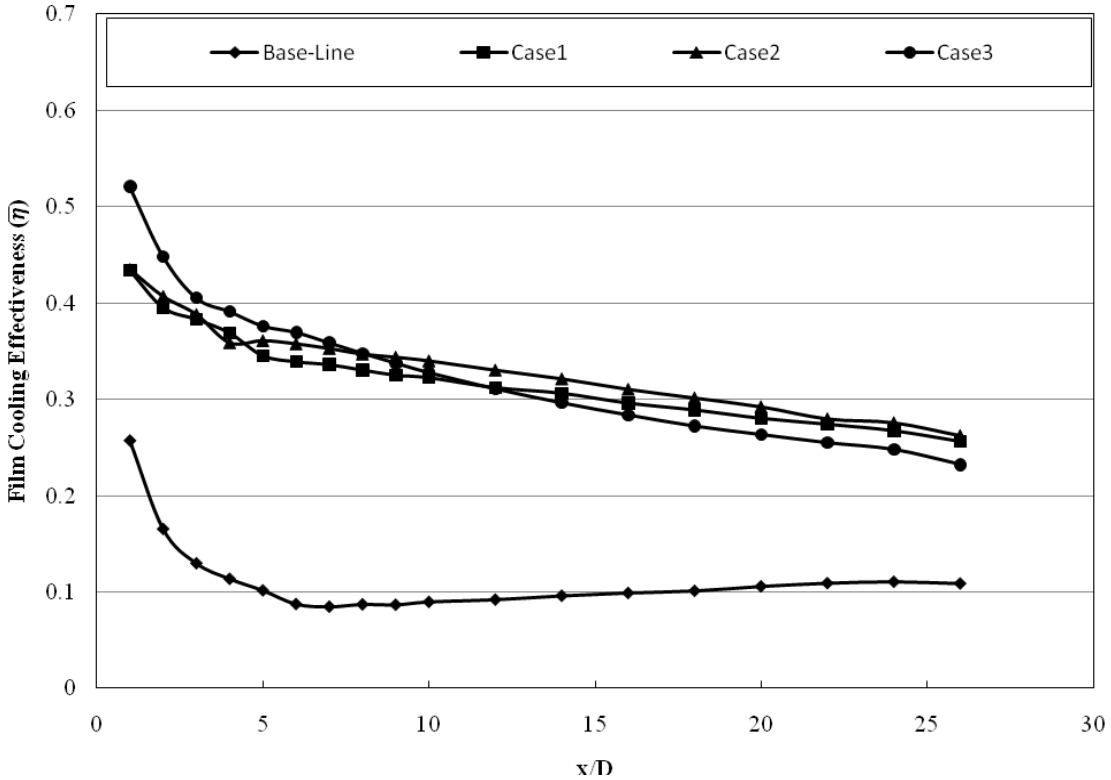


a) Under ZPG

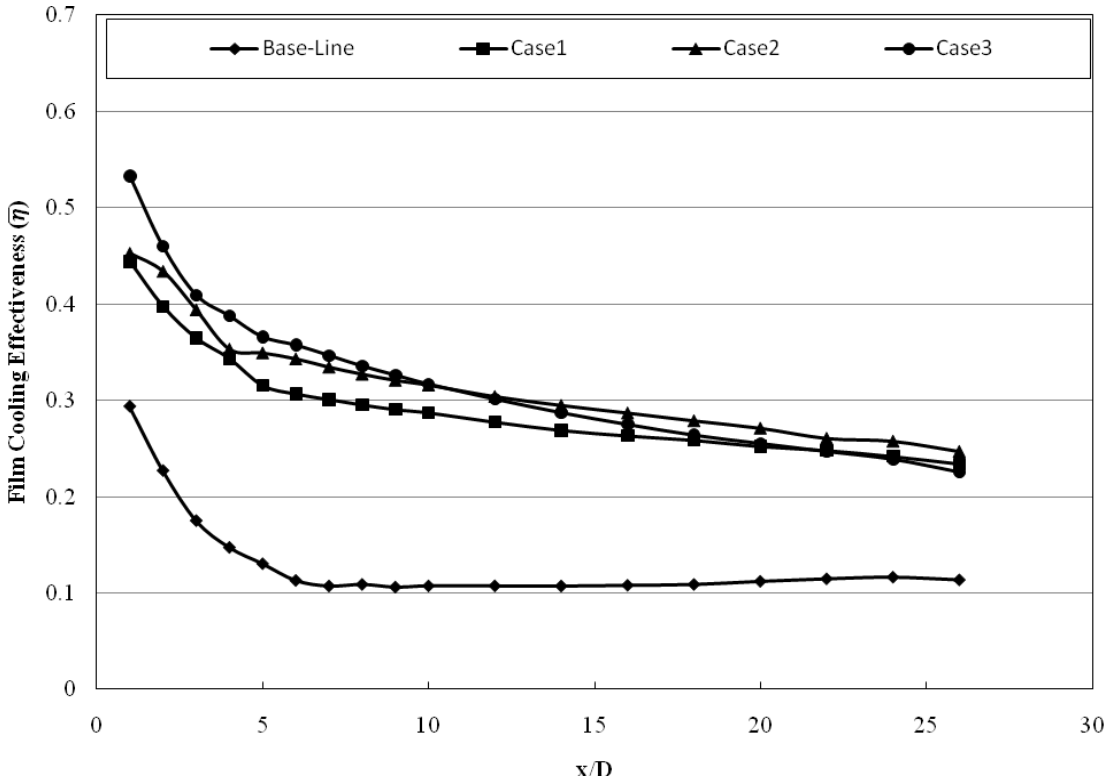


b) Under APG(1)

Figure (6.6) Spanwise Averaged Film Cooling Effectiveness Distributions under ZPG and APG(1) at VR = 1.0 (Numerical)

For VR = 1.5, figure (6.7) shows that, the baseline film cooling effectiveness has the same trend as the baseline film cooling effectiveness for VR = 1.0 but with lower values for both ZPG and APG(1).

For ZPG, case 1 and 2 give the same spanwise film cooling effectiveness with small decreasing as moving away from the film holes. For APG(1), case 1 and 2 gives the same trend as ZPG but with lower values of film cooling effectiveness. The drop in film cooling effectiveness due to APG(1) in case 1 is more than that in case 2. For case 3, the film cooling effectiveness decreases rapidly as moving away from the film holes for both ZPG and APG(1). Under APG(1), case 3 gives the highest film cooling effectiveness before x/D = 5.

For VR = 2.0, figure (6.8) shows that, the baseline film cooling effectiveness has the same trend as compared with VR = 1.0 and 1.5 but with lower values for both ZPG and APG(1). Case 1 under ZPG gives the highest film cooling effectiveness while under APG(1) case 2 gives the highest film cooling effectiveness. For both case 1 and case 2 under both ZPG and APG(1), the film cooling effectiveness may be assumed to be constant along the studied area. Case 3 shows a rabid decrease in film cooling effectiveness as moving away from the film holes although it gives the highest film cooling effectiveness just downstream the film holes.

From the above results, for baseline case, the momentum ratio increases with high velocity ratios, so the coolant jet has the ability to penetrate the mainstream flow. According to that, at high velocity ratios, the film cooling effectiveness starts from high value at the film cooling hole and suddenly decreases as moving away from the film cooling hole then starts to increase gradually as the jet flow mixes with the mainstream flow. For anti-vortex cases, the jet flow distributes through the main hole and the anti-vortex holes. In cases 1 and 2, the flow from the anti-vortex holes is moving above the flow from the main hole and is trying to mitigate it to move beside the test surface. But in case 3, the flow from the anti-vortex holes is moving inline with the flow from the main hole. So, in case 3, the film cooling effectiveness start from the highest value but it decreases rabidly as compared with case1 and 2.

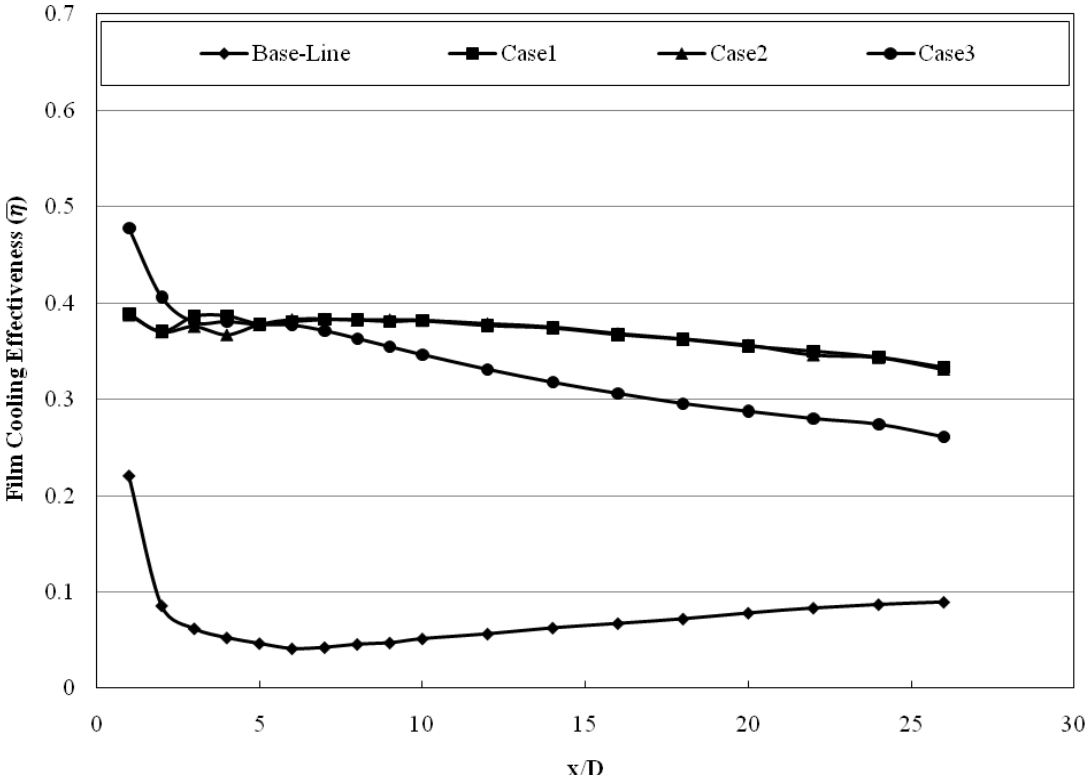


a) Under ZPG

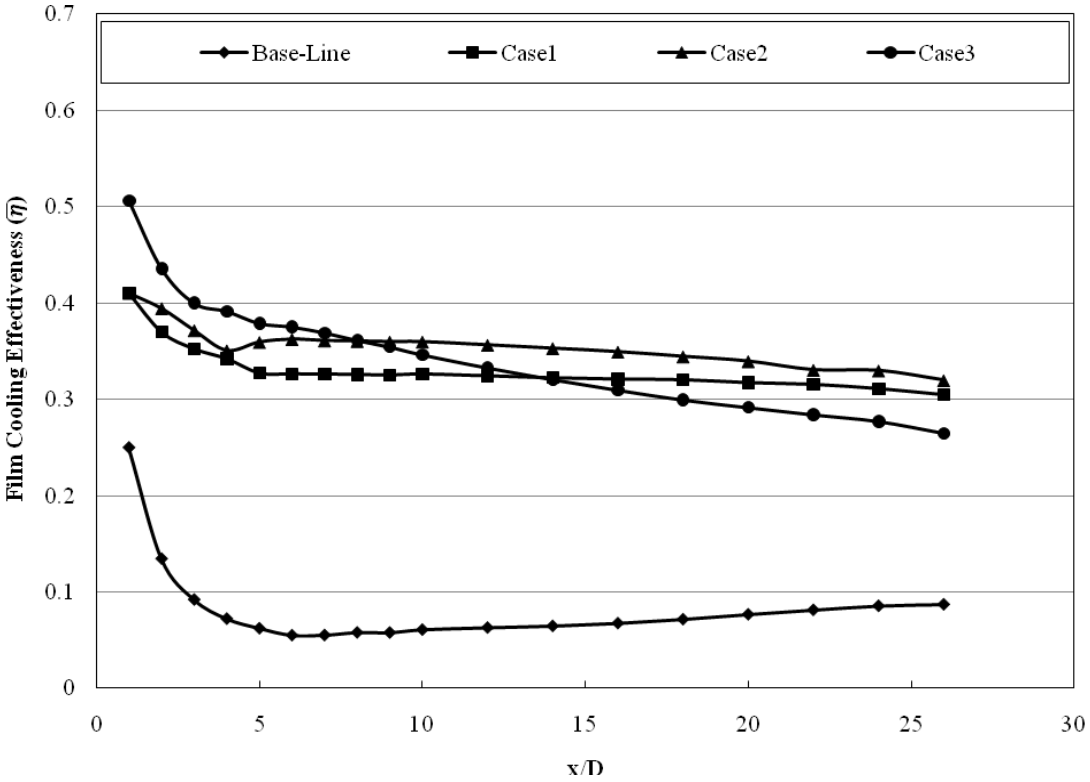


b) Under APG(1)

Figure (6.7) Spanwise Averaged Film Cooling Effectiveness Distributions under ZPG and APG(1) at VR = 1.5 (Numerical)

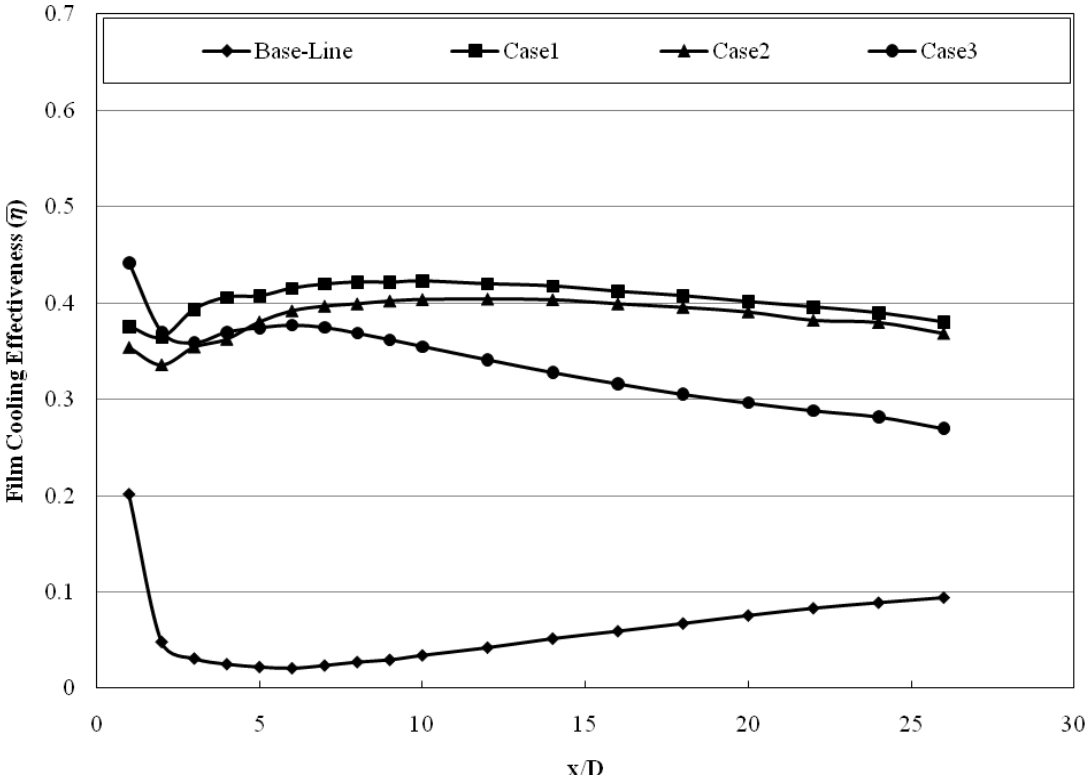


a) Under ZPG

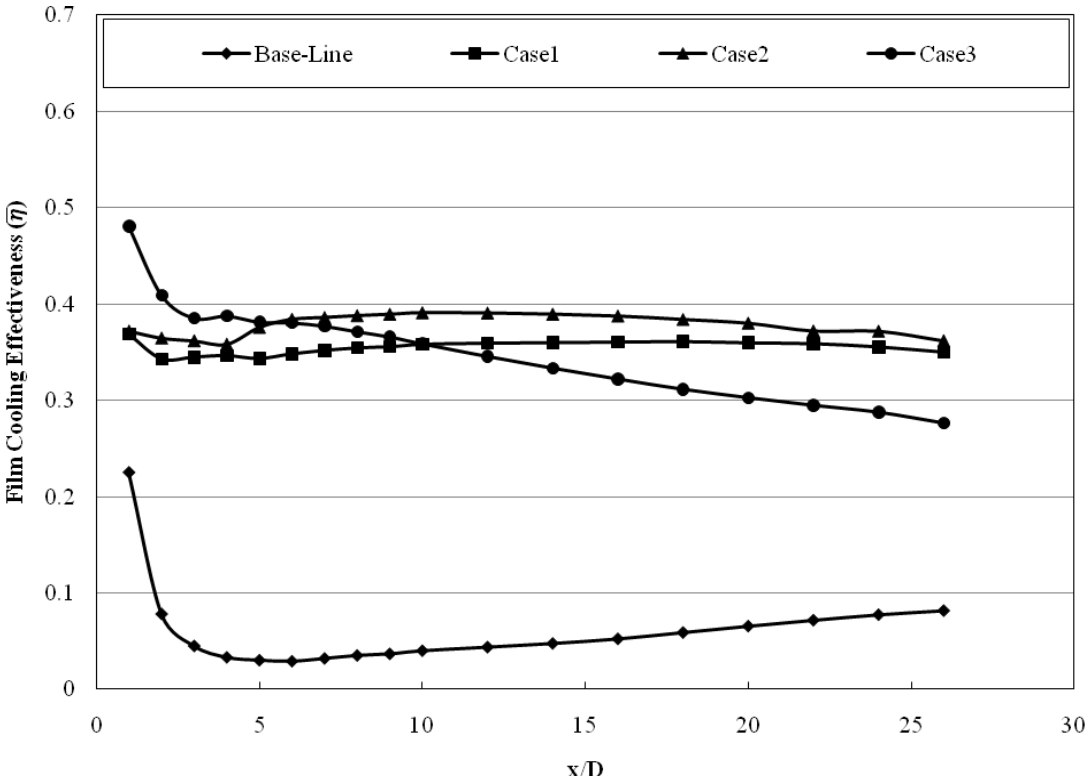


b) Under APG(1)

Figure (6.8) Spanwise Averaged Film Cooling Effectiveness Distributions under ZPG and APG(1) at VR = 2.0 (Numerical)

### 6.1.3 Overall Area Averaged Film Cooling Effectiveness

The overall area averaged film cooling effectiveness is calculated for the area downstream the middle hole only. The calculate area limits are (x/D =0 to x/D = 25, and z/D = -1.5 to z/D = 1.5 for y/D =0).

Figure (6.9) shows the overall area averaged film cooling effectiveness for all studied cases under ZPG and APG(1) with different values of velocity ratios. The figure shows that:

For baseline, as the velocity ratio increases, the overall film effectiveness decreases for both ZPG and APG(1) because with the low velocity ratios the jet flow is moving beside the test surface while with the high velocity ratios the jet flow is penetrating the main flow and moving away from the test surface.

For case 1 and 2, for both ZPG and APG(1), as the velocity ratio increases, the overall film effectiveness increases. The flow through the anti-vortex holes is taken from the flow through the main hole which reduces the velocity ratio in the main hole and keeping the flow from the main hole near the test surface. The flow from the anti vortex holes is also trying to mitigate the flow from the main hole. As the velocity ratio increases, the mitigation effect due to the anti-vortex holes flow increases. Case 1 gives the highest overall effectiveness at VR = 2.0 while for low Velocity Ratio (VR = 0.5), case 3 gives the highest effectiveness. Under APG(1), case 2 gives the highest overall film effectiveness for VR = 2 with a significant different as compared with case 1.

Case 3 gives higher overall film cooling effectiveness as compared with baseline case. Case 3 gives the highest overall film cooling effectiveness at low velocity ratio. At higher velocity ratios, the overall area averaged film cooling effectiveness for case 3 may be assumed constant. In case 3, the flow from the anti-vortex holes is moving beside the flow from the main hole and doesn’t try to mitigate the flow from the main hole.

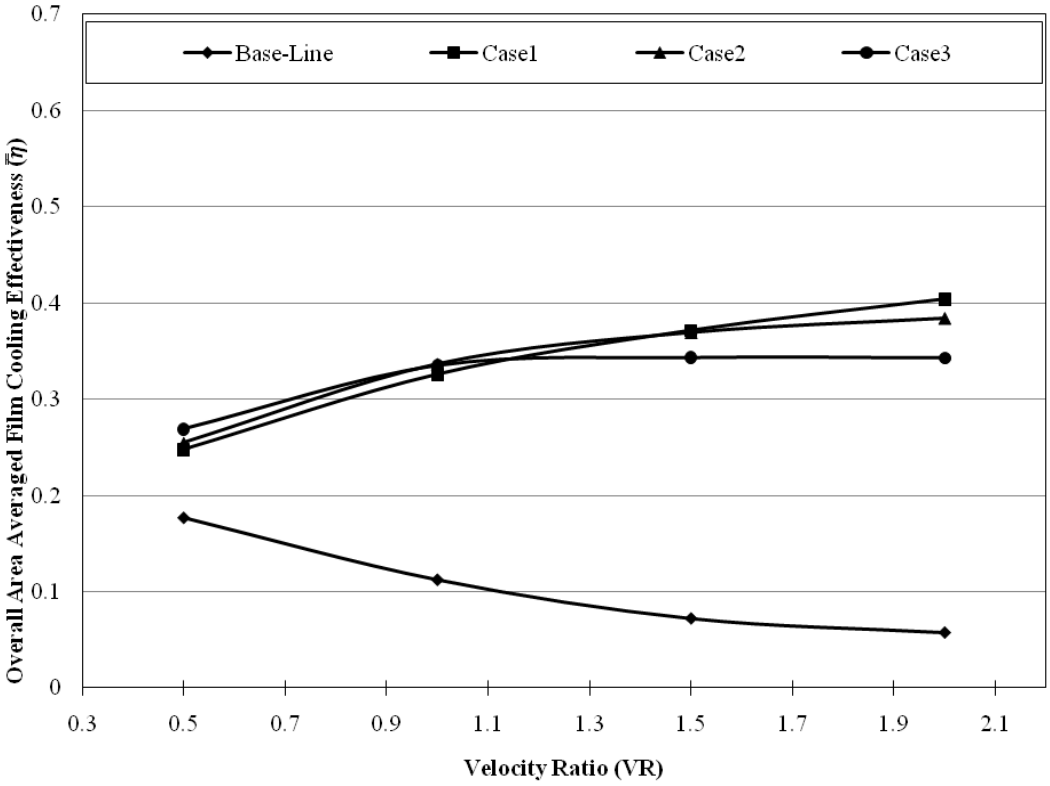


a) Under ZPG

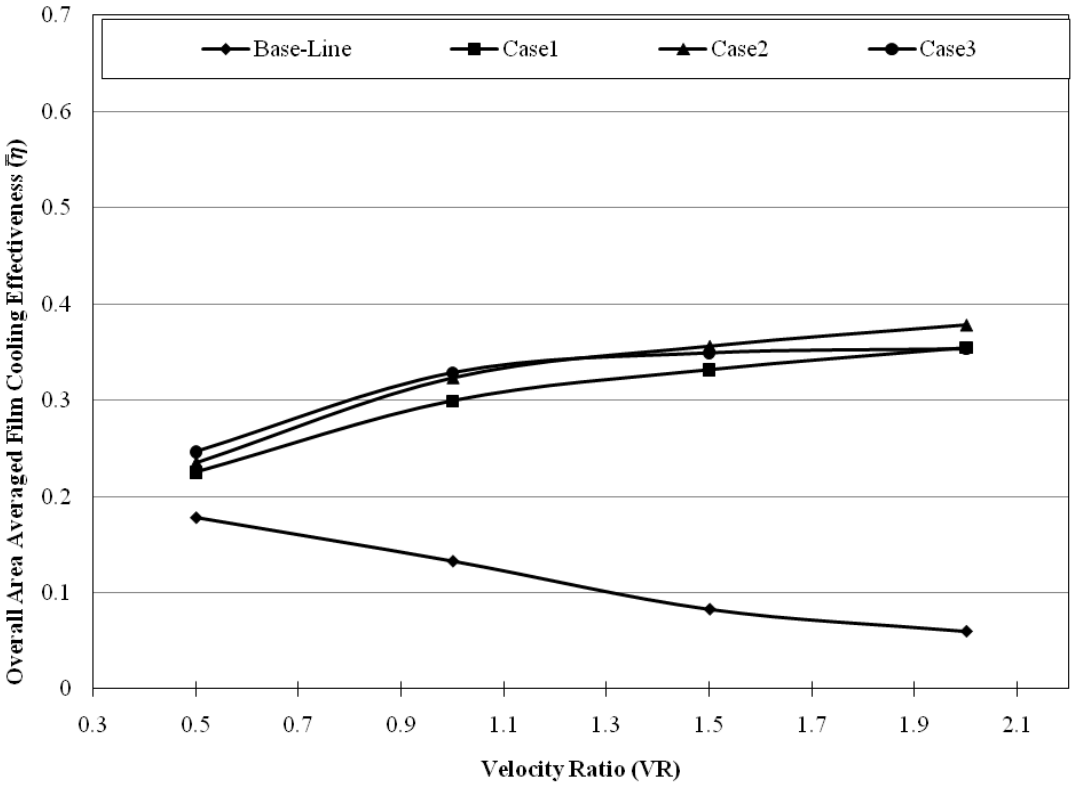


b) Under APG(1)

Figure (6.9) The overall area averaged film cooling effectiveness under ZPG and APG(1) at different velocity ratios (Numerical)

## 6.2 Experimental Results

The measured mainstream velocity using standard three holes Pitot tube is 8.6 m/s in all studied cases. The mainstream Reynolds number ($Re_x$) based on the distance measured from the trip wire to the film hole center was 452,744. Four velocity ratios, VR=0.5, 1.0, 1.5 and 2.0, are used for the 30° baseline case, case(1), case (2), and case (3). The corresponding blowing ratio (BR), momentum flux ratio (MR), and injectant Reynolds number ($Re_D$) are presented in table (6.1). All experiments were taken when atmospheric temperature was ranged from 17 to 20 $^oC$. And the presented data in table 6.1 was calculated at 18 $^oC$. The coolant to mainstream density ratio for the present test is close to 0.94.All results are presented at the middle hole only.

Table (6.1) The Blowing Ratio, Momentum Flux Ratio, and Injectant Reynolds number corresponding to the studied Velocity ratios

| VR | BR | MR | $Re_D$ |
|---|---|---|---|
| 0.5 | 0.543 | 0.313 | 2929 |
| 1.0 | 0.991 | 1.044 | 5347 |
| 1.5 | 1.45 | 2.09 | 7562 |
| 2.0 | 1.99 | 4.18 | 10695 |

### 6.2.1 Spanwise Averaged Film Cooling Effectiveness

Figures (6.10), (6.11), (6.12), and (6.13) show the experimental results for the spanwise averaged film cooling effectiveness distribution at VR = 0.5, 1.0, 1.5, and 2.0, respectively.

For VR = 0.5, figure (6.10) shows that Case 1 and Case 2 under ZPG give the highest film effectiveness along the test surface. But the film cooling effectiveness under APG(1) is lower than that under ZPG for all cases except the case 3. Any way all cases have the same trend and close to each other

because with VR = 0.5, the momentum flux of the coolant jet is lower than that of the mainstream.

For VR = 1.0, figure (6.11) shows that baseline has a different trend as compared with other cases. It starts with a high value then decreases rapidly until x/D = 6 after which, the film cooling effectiveness increases slightly again. As the adverse pressure is applied on baseline, it gives higher film cooling effectiveness as compared by ZPG but with the same trend.

Case 1 and case 2 under ZPG and APG(1) have the same trend (as the coolant fluid is moving downstream the film holes, the film cooling effectiveness decreases gradually). For case 3, as the coolant fluid is moving downstream the film holes, the film effectiveness decreases rapidly. The highest film effectiveness along the test surface, with VR = 1.0, is given by case 2. Under APG(1), the spanwise average film cooling effectiveness is lower than that is given under ZPG for case 1 and case 2, but it is higher than that is given under ZPG for baseline and case 3.

For VR = 1.5, Figure (6.12) shows that case 1 and case 2 under ZPG and APG(1) appear to have constant values of film cooling effectiveness along the test surface but with different values of each case. Case 1 and Case 2 are close to each other under ZPG and APG(1). But under APG(1), the film cooling effectiveness is lower than that is given under ZPG.

For case 3, the film effectiveness appears to start from a high value and decreases rapidly as the coolant jet fluid is moving downstream the film holes.

For VR = 2.0, figure (6.13) shows that all cases under ZPG and APG(1) still give the same trend as compared by that is given by VR = 1.5. The highest spanwise averaged film cooling effectiveness is given by case 1 under ZPG. But under APG(1), case 2 gives the highest spanwise averaged film cooling effectiveness.

For case 3, the film effectiveness that is given under ZPG and APG(1) is close to each other. The lowest film effectiveness is given by the baseline under ZPG.

From the above experimental results, the trend of the spanwise film cooling effectiveness over the test surface is similar to that is given by the numerical results. In Baseline case, the jet flow is moving beside the test surface at low velocity ratios. So, the film cooling effectiveness begins with a high value and start to decrease gradually as x/D increases. While at high velocity ratios, the jet flow penetrate the mainstream flow which lift off the jet away from the test surface.

In anti-vortex cases, the flow from the anti-vortex holes mitigates the flow from the main holes and keeping it near the test surface in case 1 and 2. While in case 3, the flow from the anti-vortex holes is moving beside the flow from the main hole. So, in case 1 and 2, the film cooling effectiveness may be assumed constant along the test surface while in case 3, the film cooling effectiveness decreases gradually along the test surface.

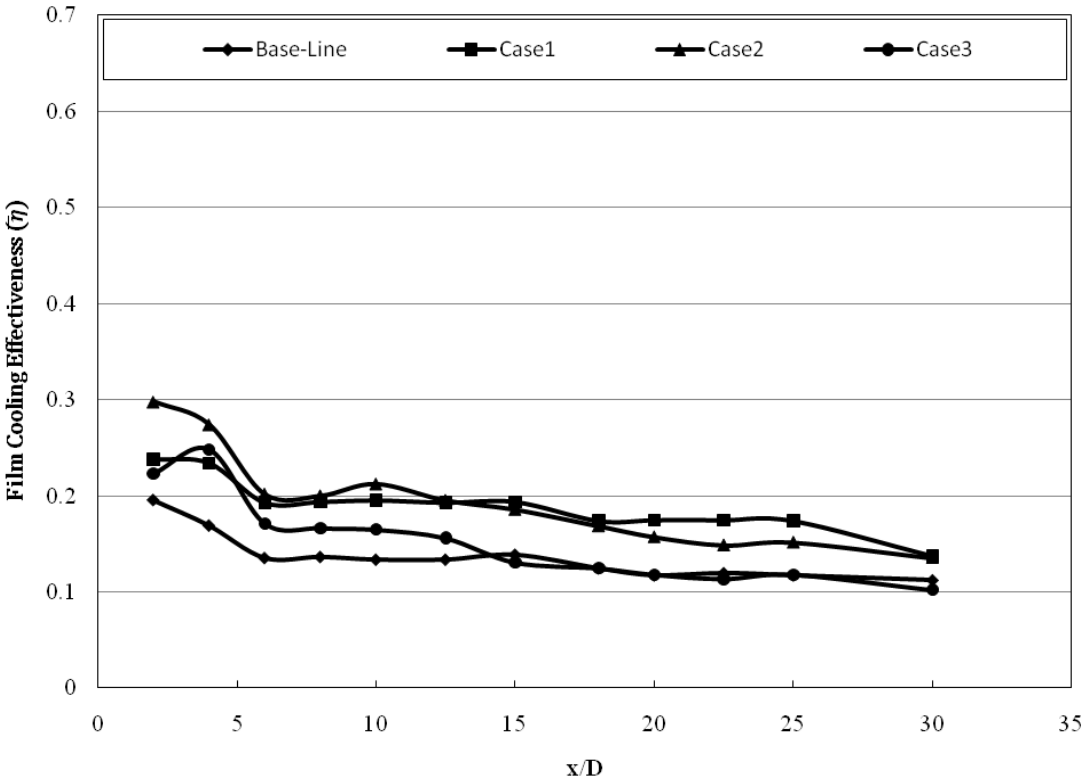


a) Under ZPG

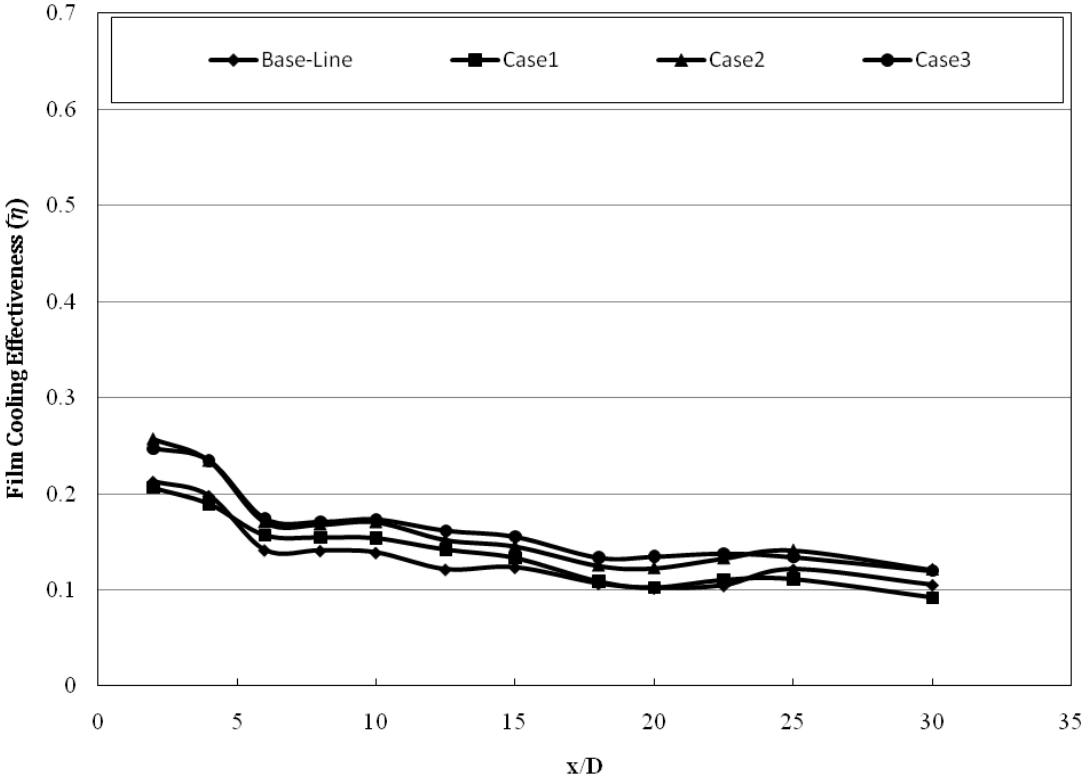


b) Under APG(1)

Figure (6.10) Spanwise Averaged Film Cooling Effectiveness Distributions under ZPG and APG(1) at VR = 0.5 (Experimental)

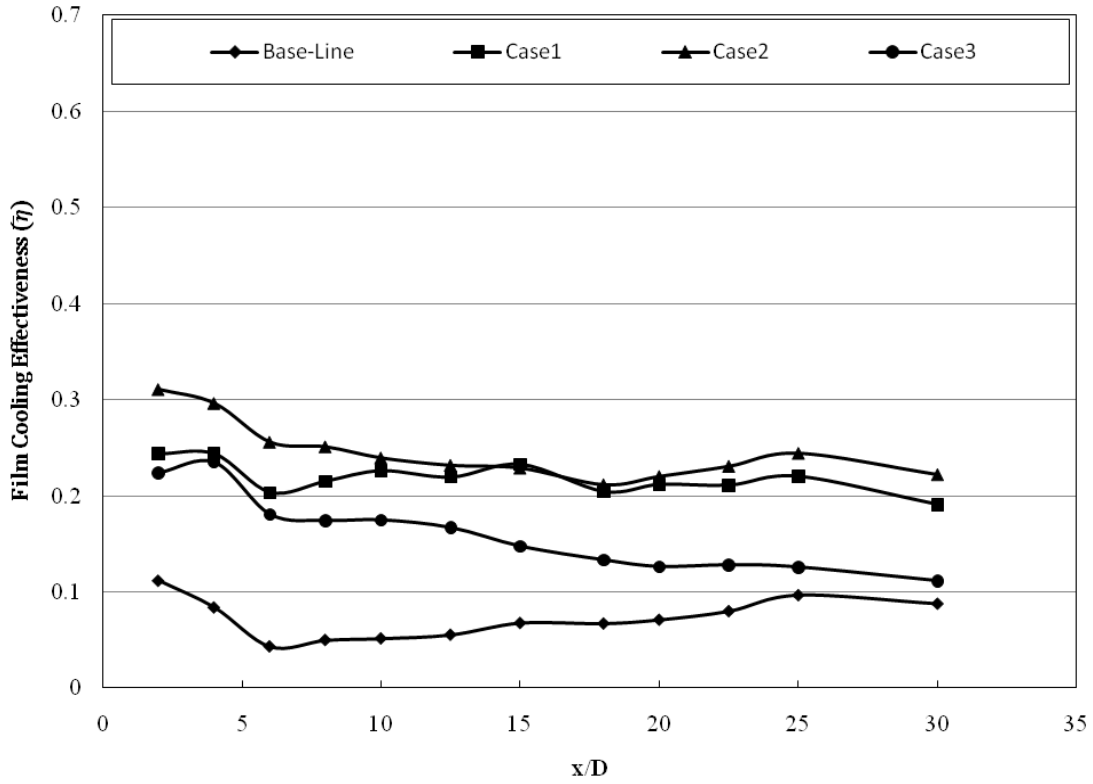


a) Under ZPG

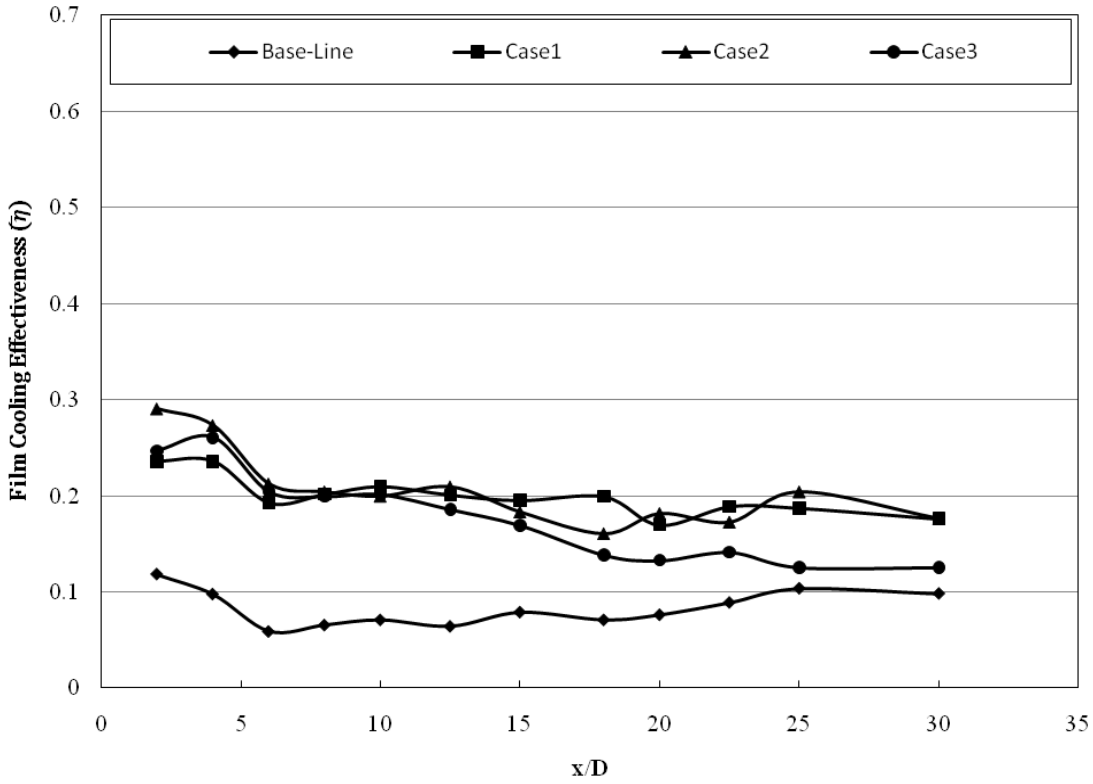


b) Under APG(1)

Figure (6.11) Spanwise Averaged Film Cooling Effectiveness Distributions under ZPG and APG(1) at VR = 1.0 (Experimental)

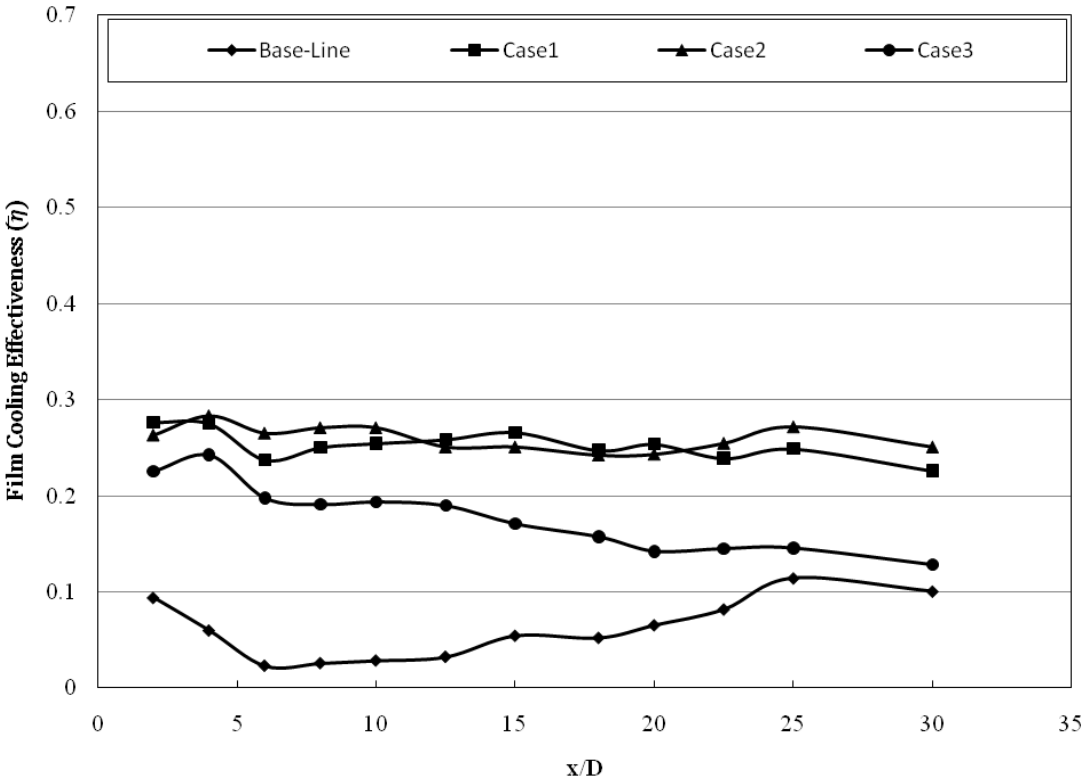


a) Under ZPG

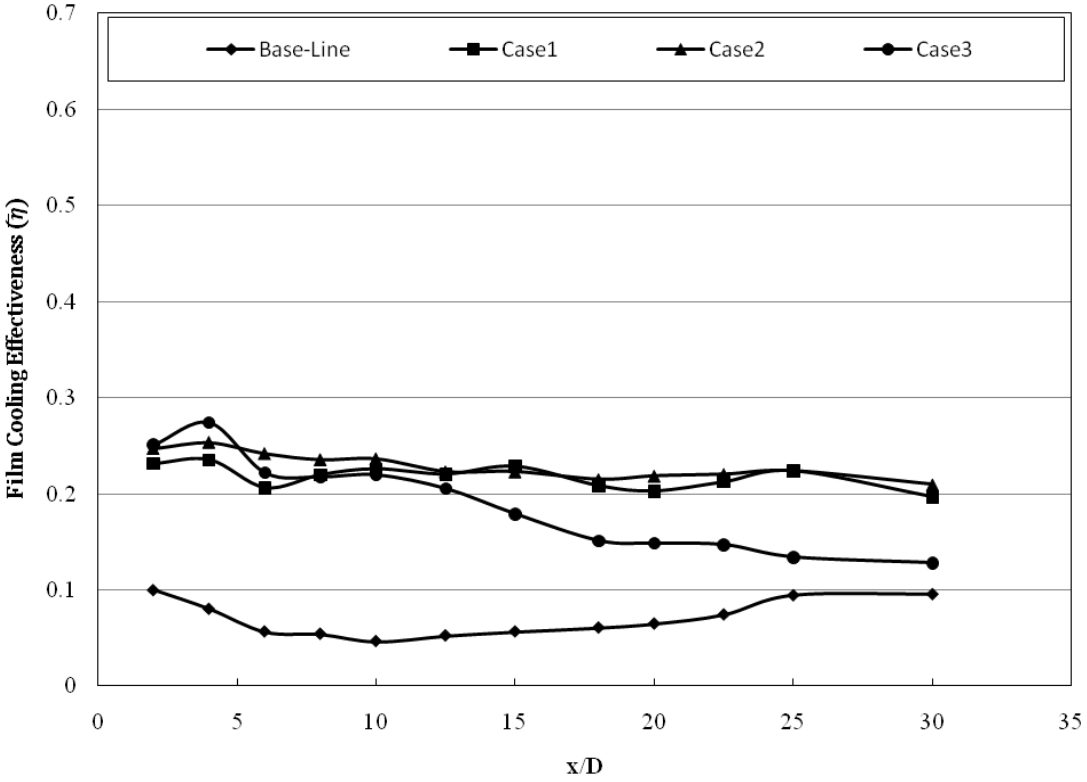


b) Under APG(1)

Figure (6.12) Spanwise Averaged Film Cooling Effectiveness Distributions under ZPG and APG(1) at VR = 1.5 (Experimental)

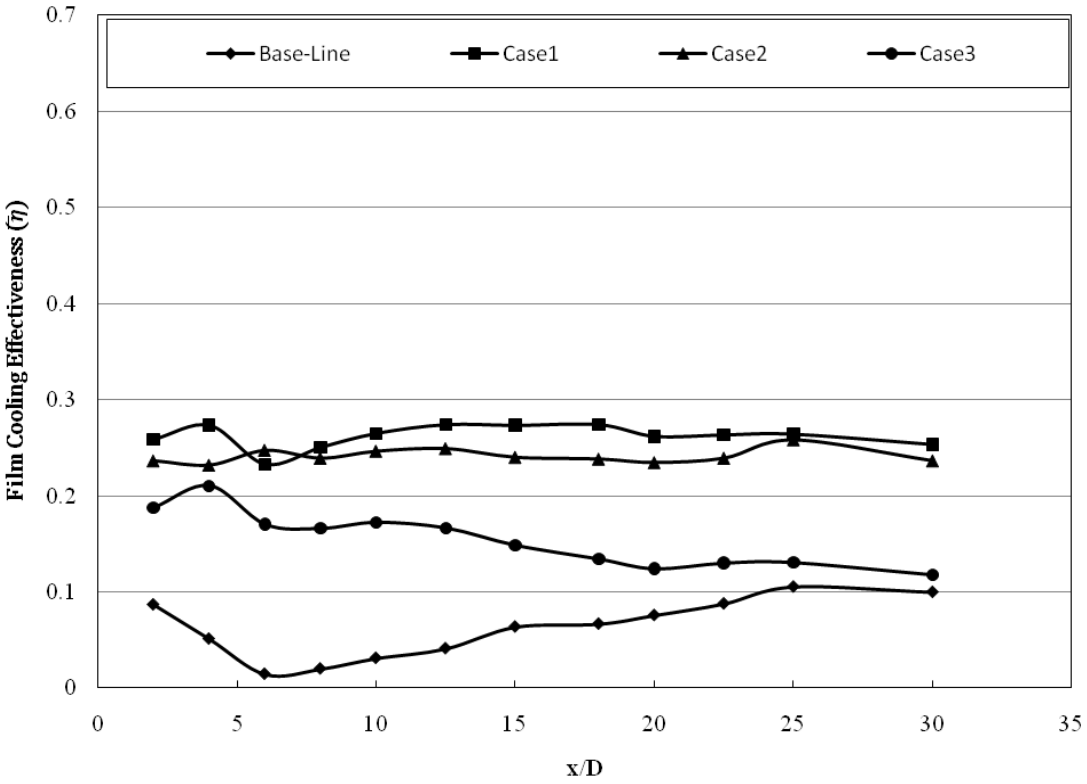


a) Under ZPG

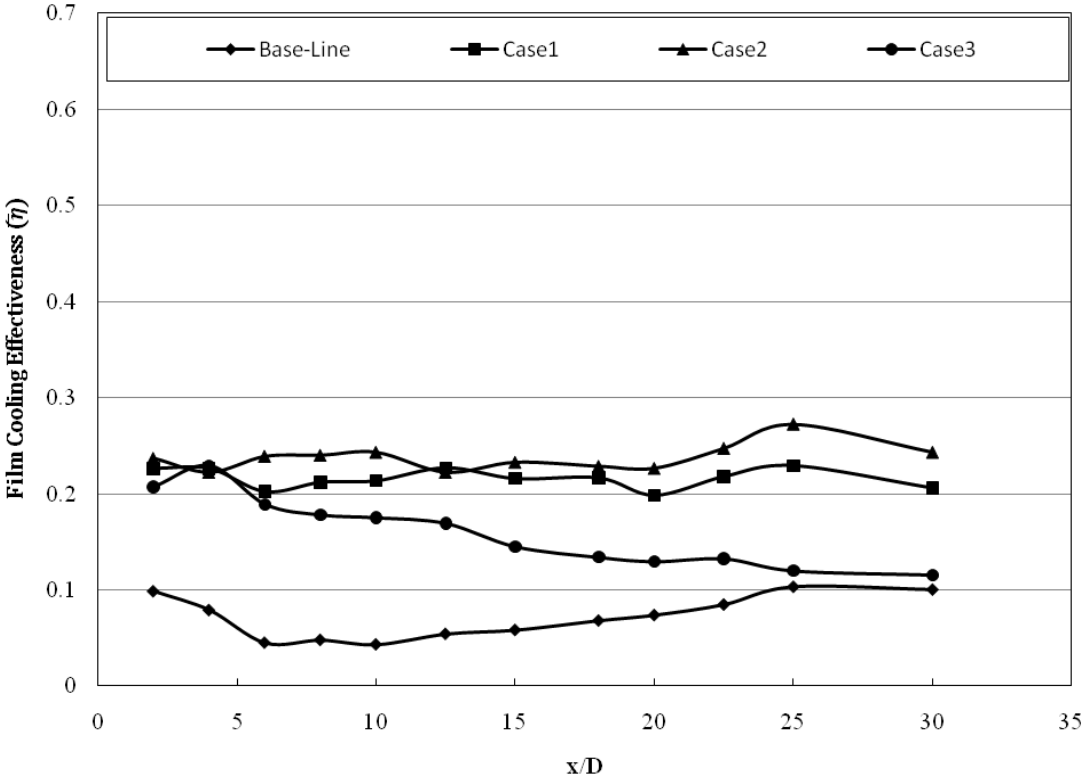


b) Under APG(1)

Figure (6.13) Spanwise Averaged Film Cooling Effectiveness Distributions under ZPG and APG(1) at VR = 2.0 (Experimental)

### 6.2.2 Overall Area Averaged Film Cooling Effectiveness

The overall area averaged film cooling effectiveness is calculated for the area downstream the middle hole only. The calculate area limits are (x/D =0 to x/D = 25, and z/D = -1.5 to z/D = 1.5 for y/D =0).

Figure (6.14) shows the experimental overall area averaged film cooling effectiveness for all studied cases under ZPG and APG(1) with different values of velocity ratios. The figure shows that:

For baseline under ZPG and APG(1), low velocity ratio gives a higher overall averaged area film cooling effectiveness. As the velocity ratio increases, the overall area averaged film cooling effectiveness appear to has a constant value.

For case 1 under ZPG and APG(1), as the velocity ratio increases the overall area averaged film cooling effectiveness increases. The highest overall film cooling effectiveness is given by case 1 under ZPG at VR = 2.0. For all other velocity ratios, the highest overall film effectiveness is given by case 2 under ZPG. Under APG(1), the highest overall film cooling effectiveness is given by case 2 for all velocity ratios.

The overall area averaged film cooling effectiveness with case 3 under APG(1) is higher than that under ZPG for all velocity ratios. For case 3 under ZPG and APG(1), the overall area averaged film cooling effectiveness appears to move around a constant value at all studied velocity ratios.

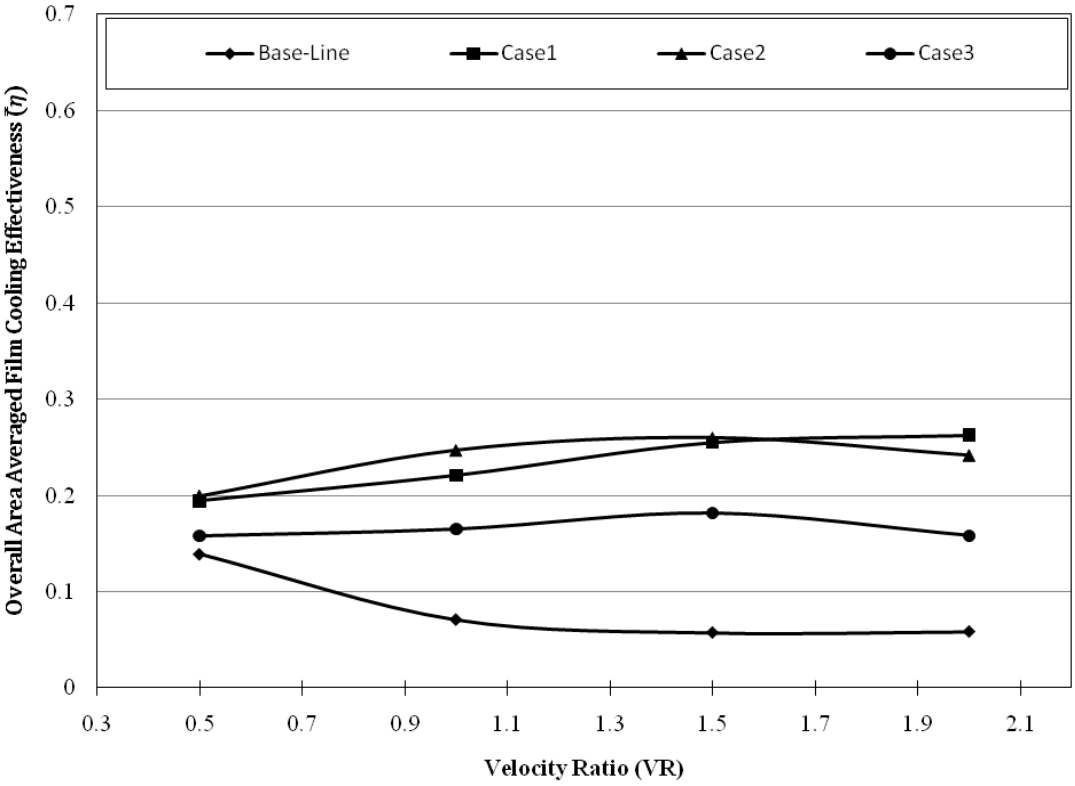


a) Under ZPG

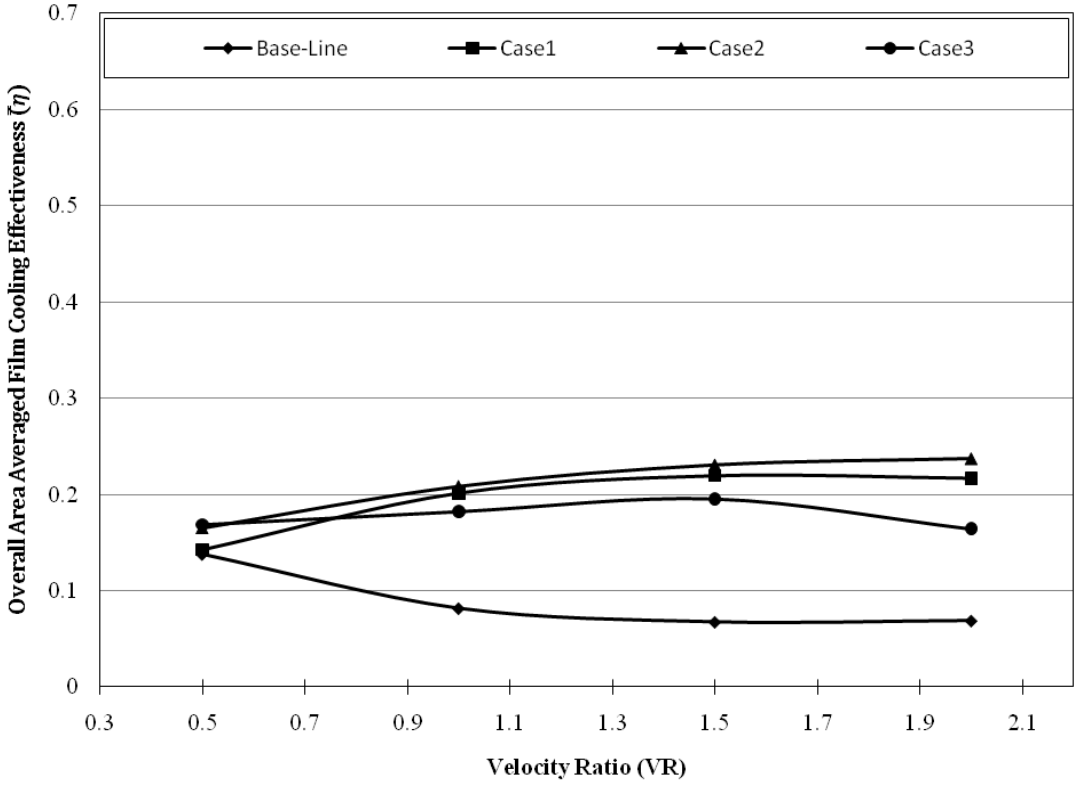


b) Under APG(1)

Figure (6.14) The overall area averaged film cooling effectiveness under ZPG and APG(1) at different velocity ratios (Experimental)

## 6.3 Comparison between Experimental and Numerical Results

In this part, a comparison sample between experimental and numerical results of the present work will be presented and also a comparison between the results of the present work and previous researches will be presented, especially for baseline which is available from previous researches.

### 6.3.1 Present Work experimental and numerical results Comparison

Figures (6.15a) and (6.15b) show the spanwise averaged film cooling effectiveness distribution under ZPG for experimental and numerical results of the present work at VR = 0.5 and VR = 2.0 respectively. The two figures show an agreement between the experimental and numerical results in trends for all studied cases.

For VR = 0.5, figure (6.15(a)) shows that the experimental results is close to that of numerical results for all studied cases. For VR = 2.0, It is interesting that the baseline experimental and CFD results almost match beyond x/D = 5, as shown in figure (6.15(b)).

As shown in Figure (6.16), the maximum deviation between the numerical and experimental results as a ratio of numerical results for the overall area averaged film cooling effectiveness is about 2.3% at VR = 2.0 and 21.7% at VR = 0.5 for baseline case. But for case 1, the maximum deviation is about 34.9% at VR = 2.0 and 21.6% at VR = 0.5.

It can be seen that computational predictions for the studied cases are much higher than for the experimental data. It has always been indicated by previous film cooling prediction studies that the CFD results cannot predict the spreading of jets accurately and over predict centerline effectiveness. The spanwise averaged results show similarities as the cross-stream direction is averaged and washes out the local discrepancies between the predictions and experiments (Yiping Lu [67]). This different between experimental and numerical results may be assumed due to the boundary condition assumptions which are used in the numerical model.

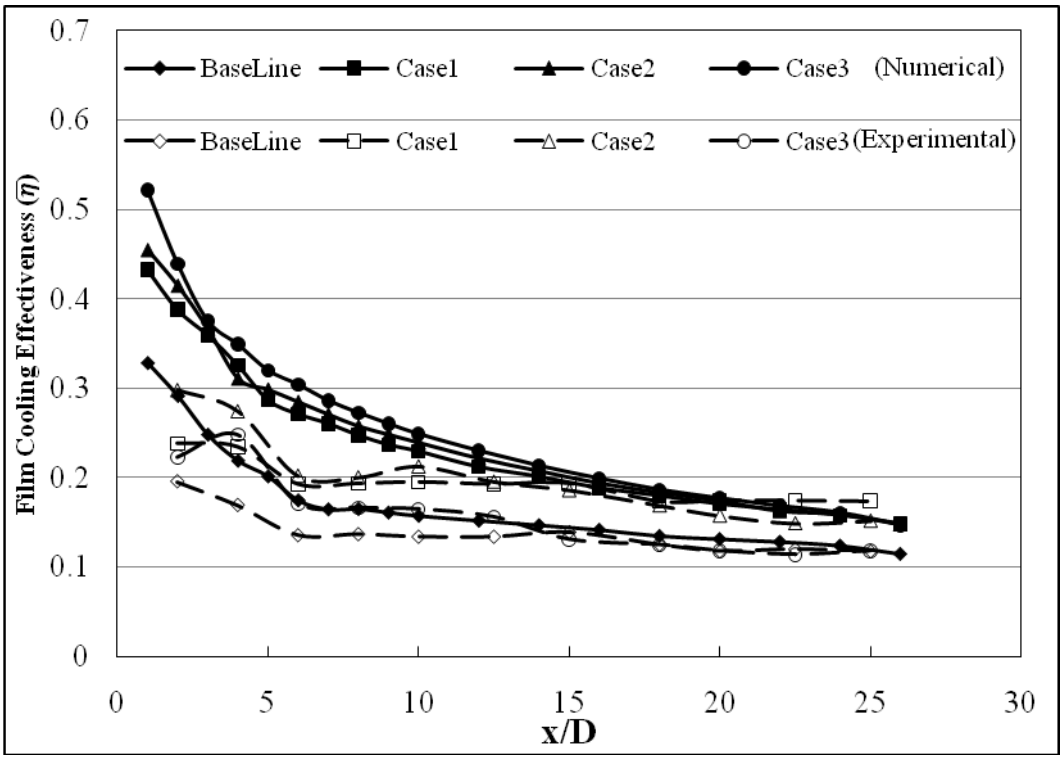


(a) VR = 0.5

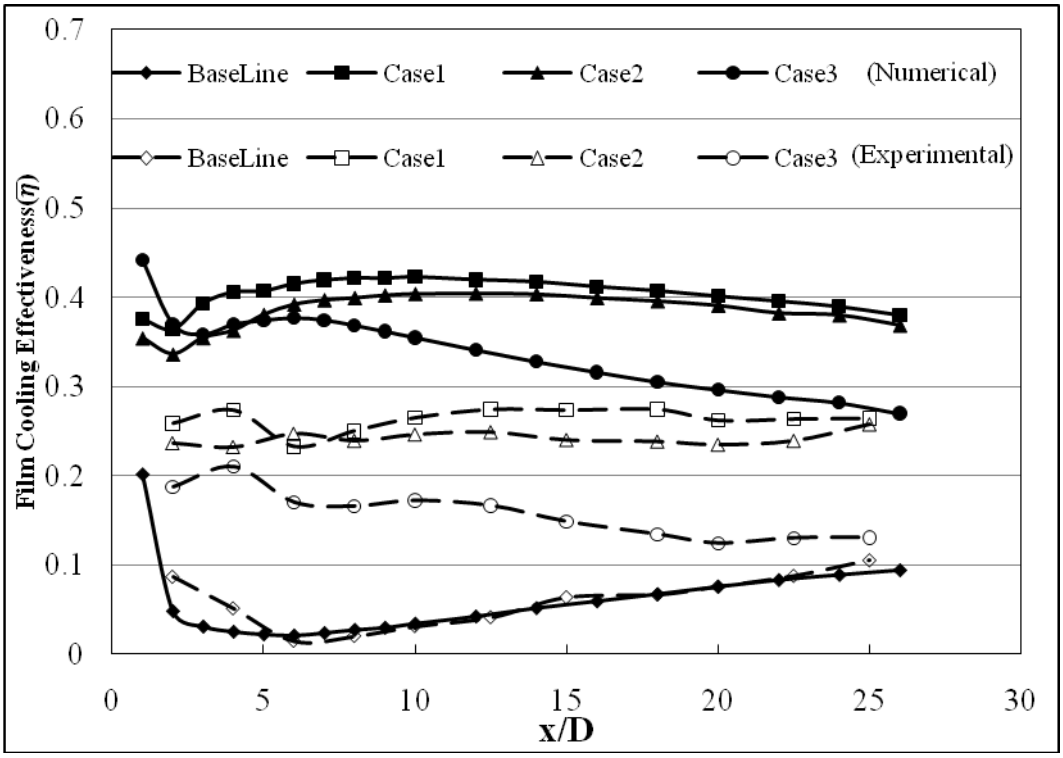


(b) VR = 2.0

Figure (6.15) Spanwise averaged film cooling effectiveness distribution under ZPG for experimental and numerical results of present work at VR = 0.5 and VR = 2.0

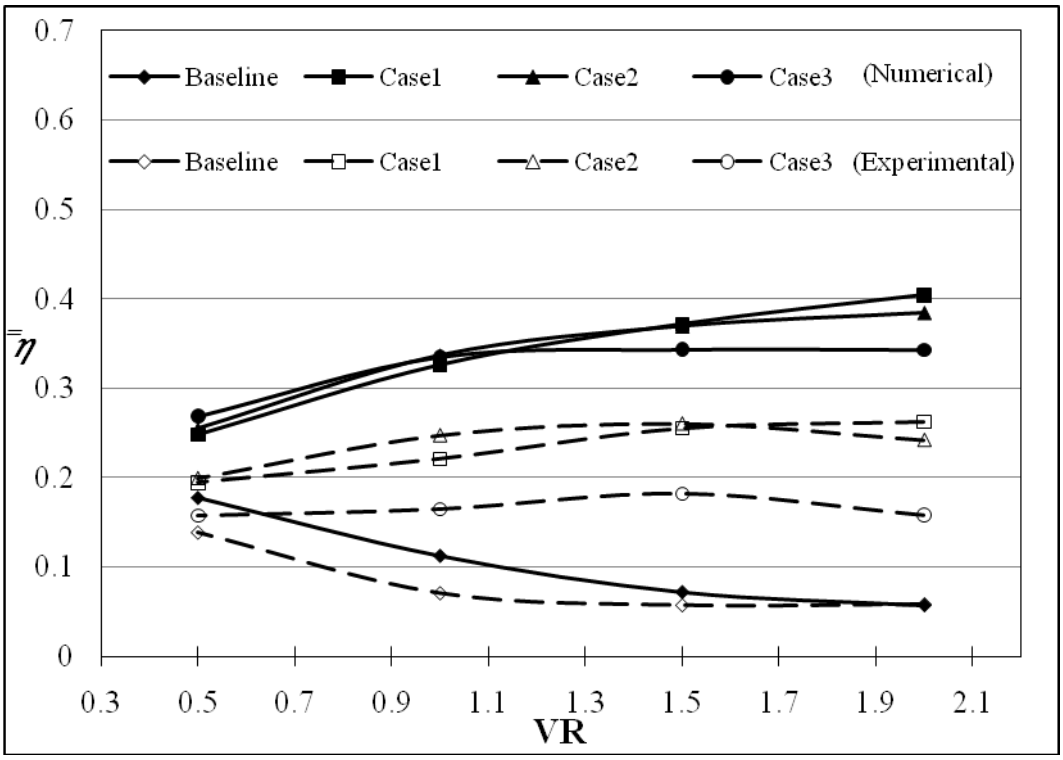


Figure (6.16) The overall averaged area film cooling effectiveness for all studied cases with different velocity ratios under ZPG

### 6.3.2 Comparison with Previous works

Figures (6.17) and (6.18) show a comparison between the present work and previous works for baseline with ZPG at VR = 0.5 and 2.0, respectively. Dhungel [11] baseline result was taken for ½ inch main hole diameter with angle of inclination equal $30^{o}$. Dhungel used infrared camera to measure the temperature distribution on the test surface. Jung et. al. [37] studied the effect of orientation angle. Their baseline was a hole with $35^{o}$ inclination angle and 20 mm diameter. They used liquid crystal technique to measure the temperature distribution.

Figures (6.19) and (6.20) show a comparison between the present work and previous works for case 1with ZPG at VR = 1.0 and 2.0, respectively. The results of Heidmann [31] were a numerical results carried out by using the 3–D Navier-Stokes solver Glenn-HT.

Figures show an agreement between the present work experimental and numerical results with experimental results of Dhungel [11] and Jung et al.[37].

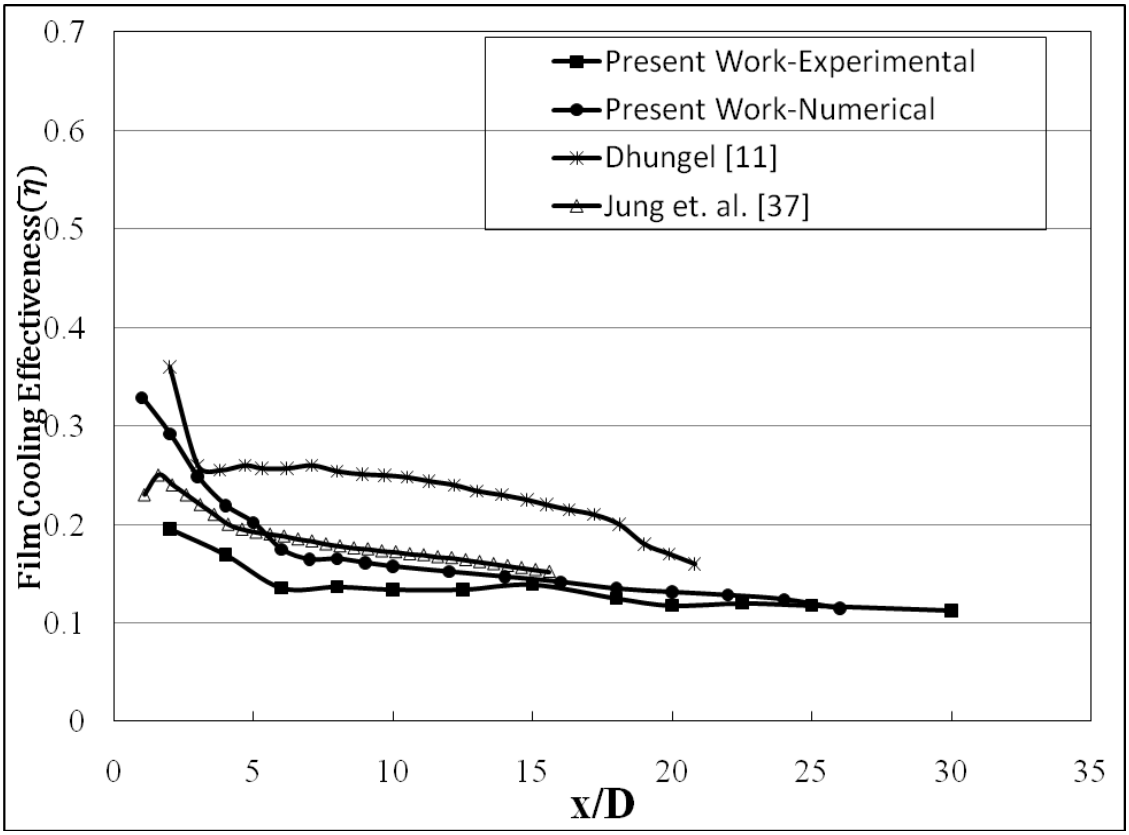


Figure (6.17) Comparison of Spanwise averaged film cooling effectiveness distribution for baseline case under ZPG, VR = 0.5

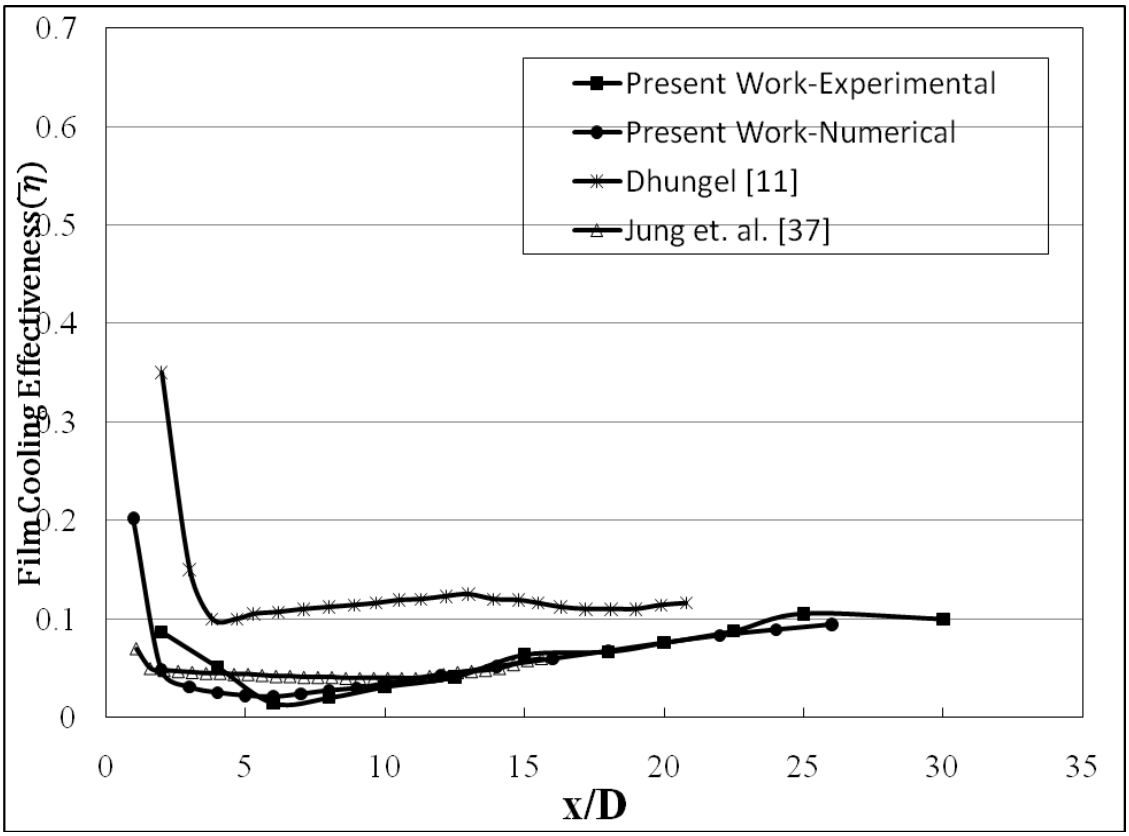


Figure (6.18) Comparison of Spanwise averaged film cooling effectiveness distribution for baseline case under ZPG, VR = 2.0

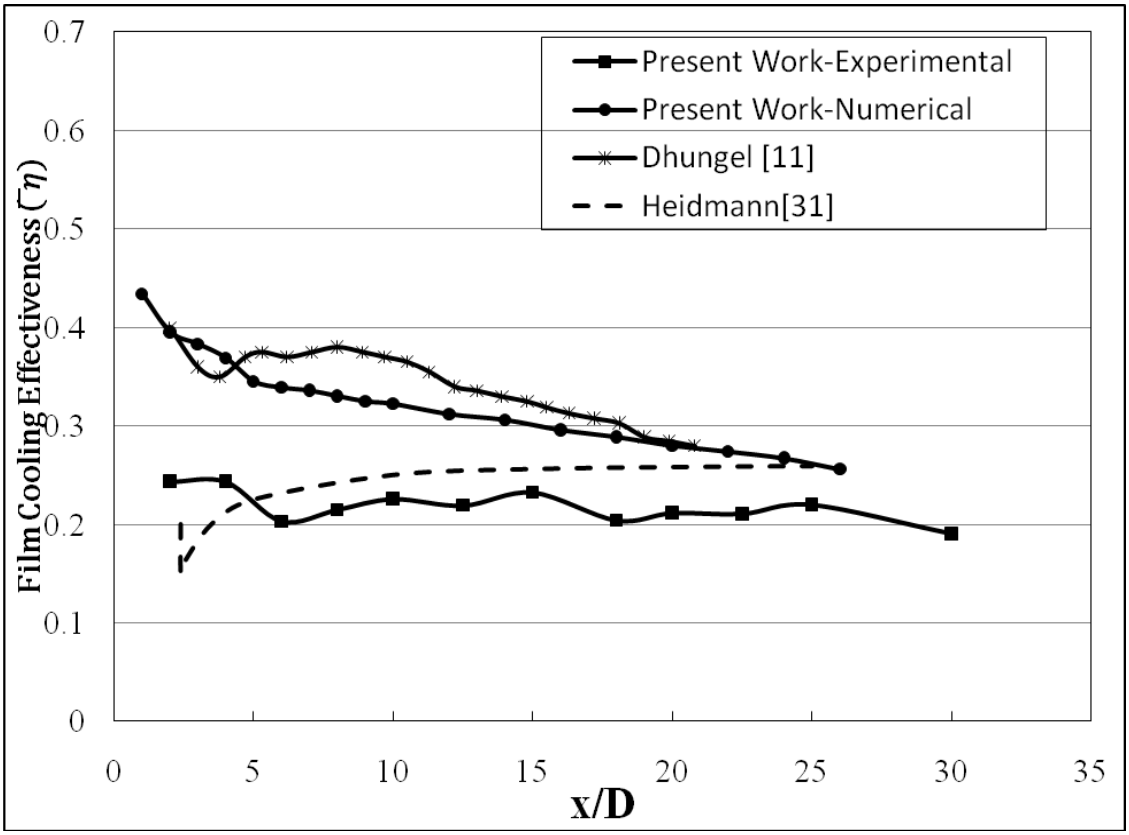


Figure (6.19) Comparison of Spanwise averaged film cooling effectiveness distribution for case 1 under ZPG, VR = 1.0

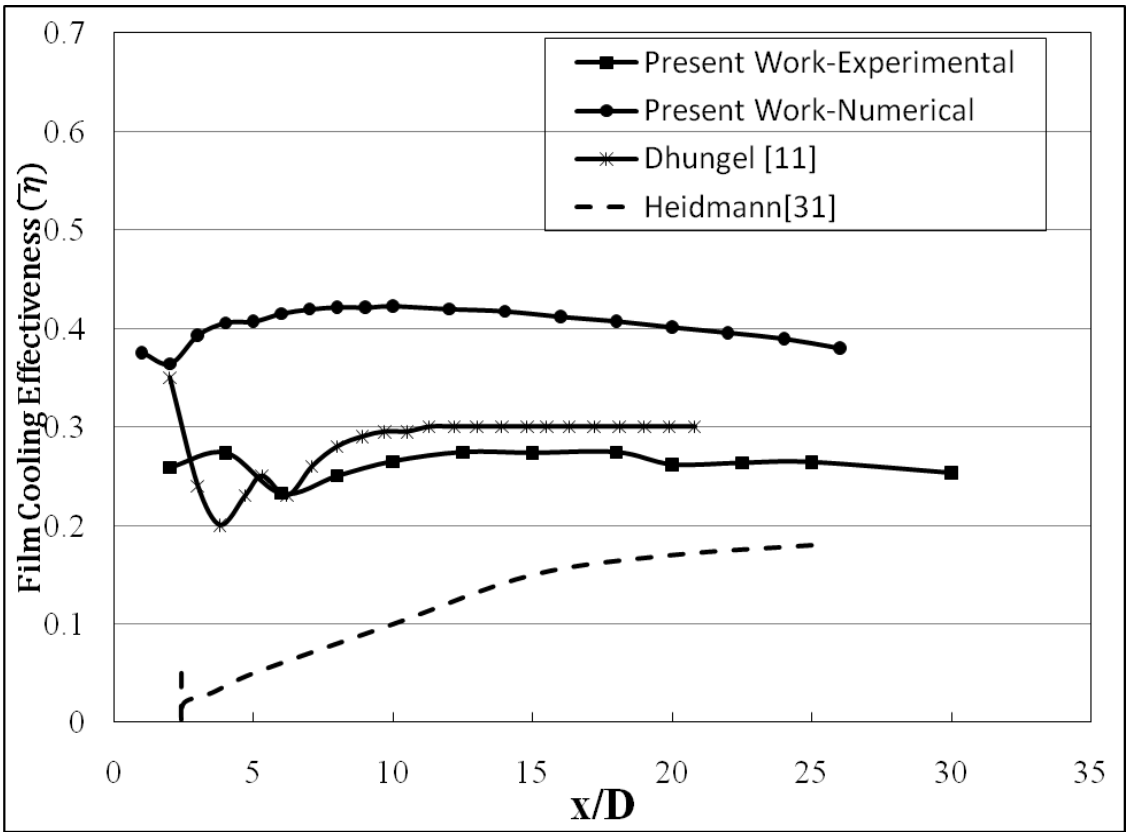


Figure (6.20) Comparison of Spanwise averaged film cooling effectiveness distribution for case 1 under ZPG, VR = 2.0

## 6.4 Effect of Different Pressure gradients

The detailed film cooling effectiveness distributions of the second studied adverse pressure gradient (APG(2)) and the favorable pressure gradient (FPG) for different studied cases are shown in Figures (6.21), (6.22), and (6.23).

At VR = 0.5, figure (6.21) shows that the favorable pressure gradient gives higher film cooling effectiveness just down the film cooling holes as compared with the second adverse pressure gradient (APG(2)). For all studied velocity ratios, the anti-vortex cases show a higher film cooling effectiveness as compared with baseline case for both adverse and favorable pressure gradients. But for the same case as the velocity ratio increases, the film cooling effectiveness increases except with the baseline case. For all studied cases, the film cooling effectiveness under FPG covers a wider area as compared with other adverse pressure gradients.

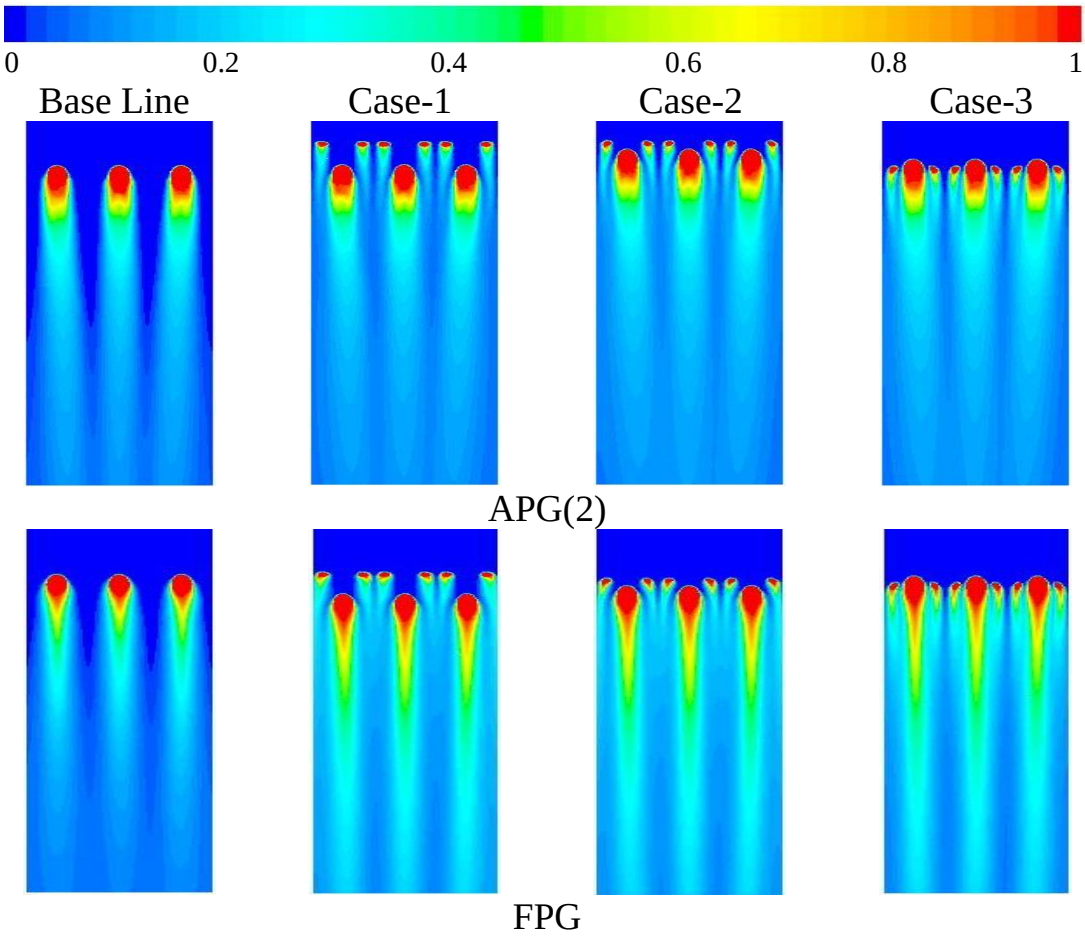


Figure (6.21) Detailed film cooling effectiveness distributions under APG(2) and FPG for different studied cases at VR = 0.5

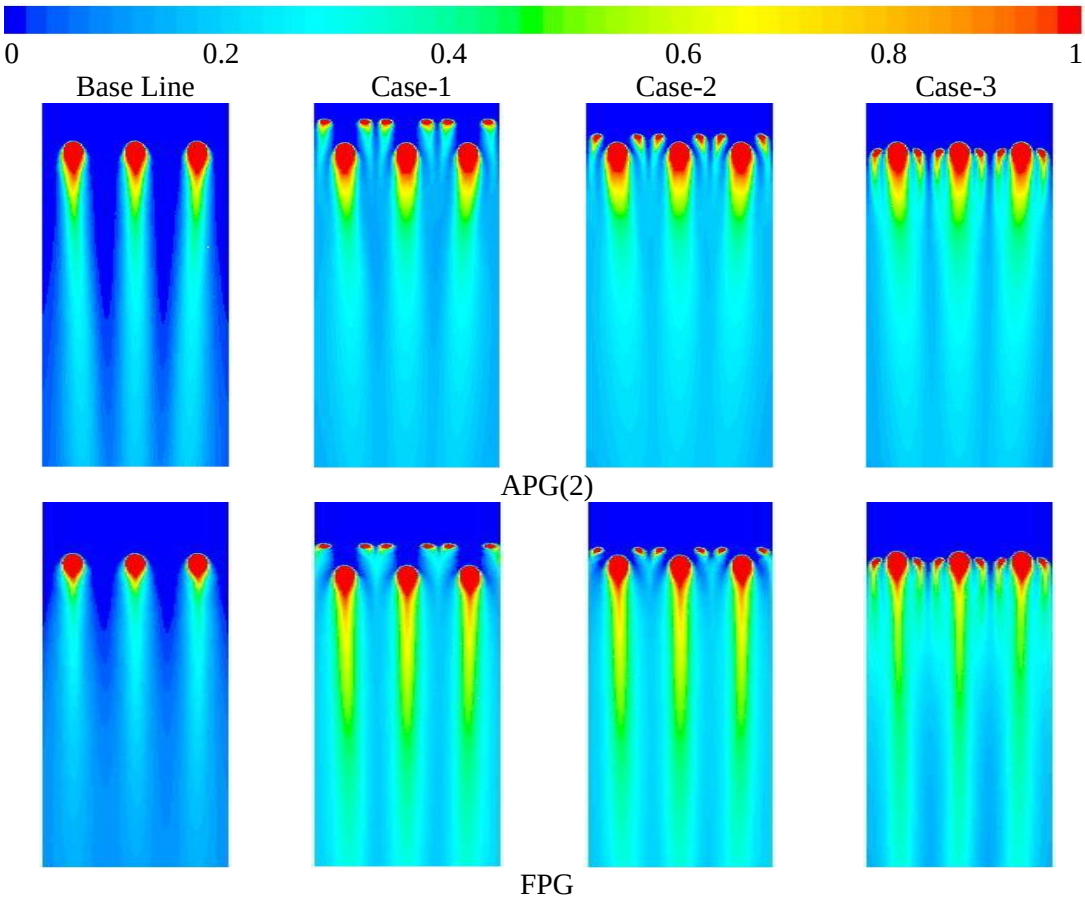


Figure (6.22) Detailed film cooling effectiveness distributions under APG(2) and FPG for different studied cases at VR = 1.0

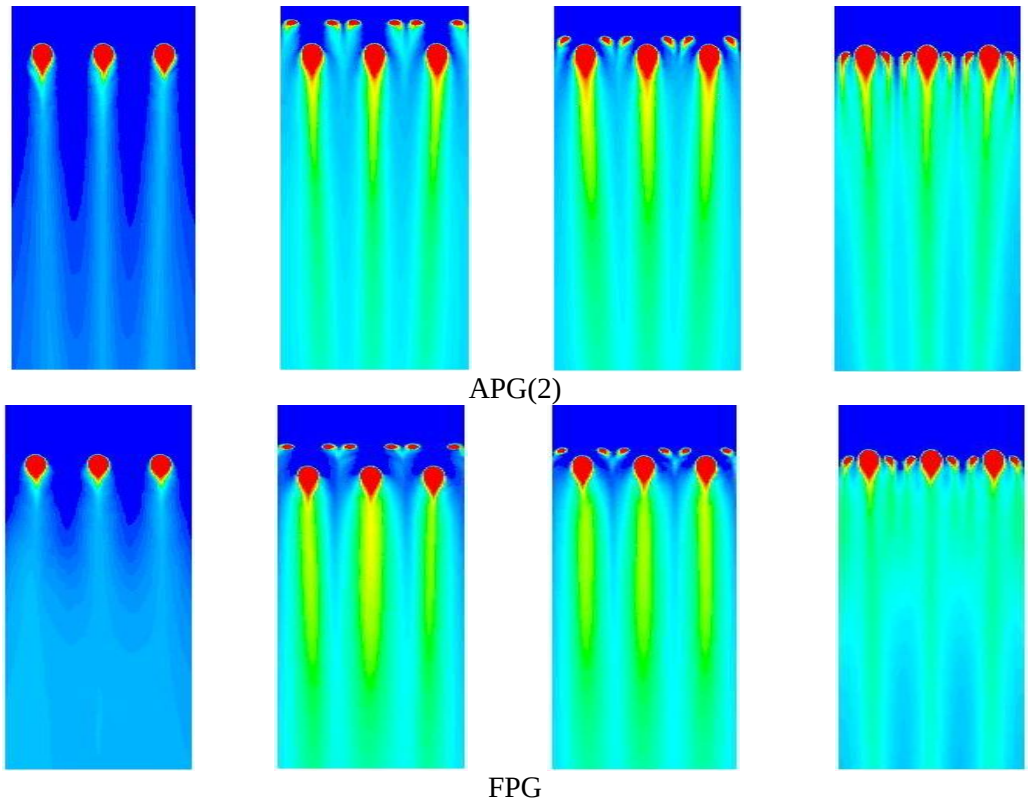


Figure (6.23) Detailed film cooling effectiveness distributions under APG(2) and FPG for different studied cases at VR = 2.0

### 6.4.1 Spanwise Averaged Film Cooling Effectiveness

Figures (6.24), (6.25), and (6.26) show the spanwise averaged film cooling effectiveness at VR = 0.5, 1.0, and 2.0, respectively under both APG(2) and FPG.

For VR = 0.5, figure (6.24) shows that the anti-vortex cases give film cooling effectiveness higher than baseline case under both APG(2) and FPG. Under FPG, the film cooling effectiveness results of anti-vortex cases are close to each other with a significant difference with the baseline case result.

For VR = 1.0, figure (6.25) shows that, under APG(2), the highest film cooling effectiveness is given by case 3, while under FPG the highest film cooling effectiveness is given by case 2. Case 1 result is close to that of case 2.

For VR = 2.0, figure (6.26) shows that, under APG(2), the highest film cooling effectiveness is given by case 3 starting just downstream the film cooling holes until x/D = 10, after which highest film cooling effectiveness is given by case 2. Under FPG, the highest effectiveness is given by case 1 with significantly different with other cases.

The film cooling effectiveness under APG(2) and FPG has the same trend as compared with the film cooling effectiveness under ZPG and APG(1). A comparison between the studied pressure gradients will be presented in details in section 6.4.3

### 6.4.2 Overall Area Averaged Film Cooling Effectiveness

Figures (6.27) and (6.28) show the overall area averaged film cooling effectiveness under APG(2) and FPG, respectively, for all studied cases with different velocity ratios.

Under APG(2), as the velocity ratio increases, the overall area averaged film cooling effectiveness decreases for baseline case while with the anti-vortex cases as the velocity ratio increases, the overall area averaged film cooling increases. The highest overall area averaged film cooling is given by case 3 for all studied velocity ratios.

Under FPG, The overall averaged area film cooling effectiveness has the same trend as compared with APG. For anti-vortex cases, the overall area averaged film cooling effectiveness results are close to each other at low velocity ratio while there is a significant difference between them at the high velocity ratio. The highest overall area averaged film cooling effectiveness is given by case 1 at VR = 2.

Favorable pressure gradient reduces the separation of cooling jet and thus causes wider contact area between the surface and the jet. Stream lines produced by FLUENT clearly explain such contact.

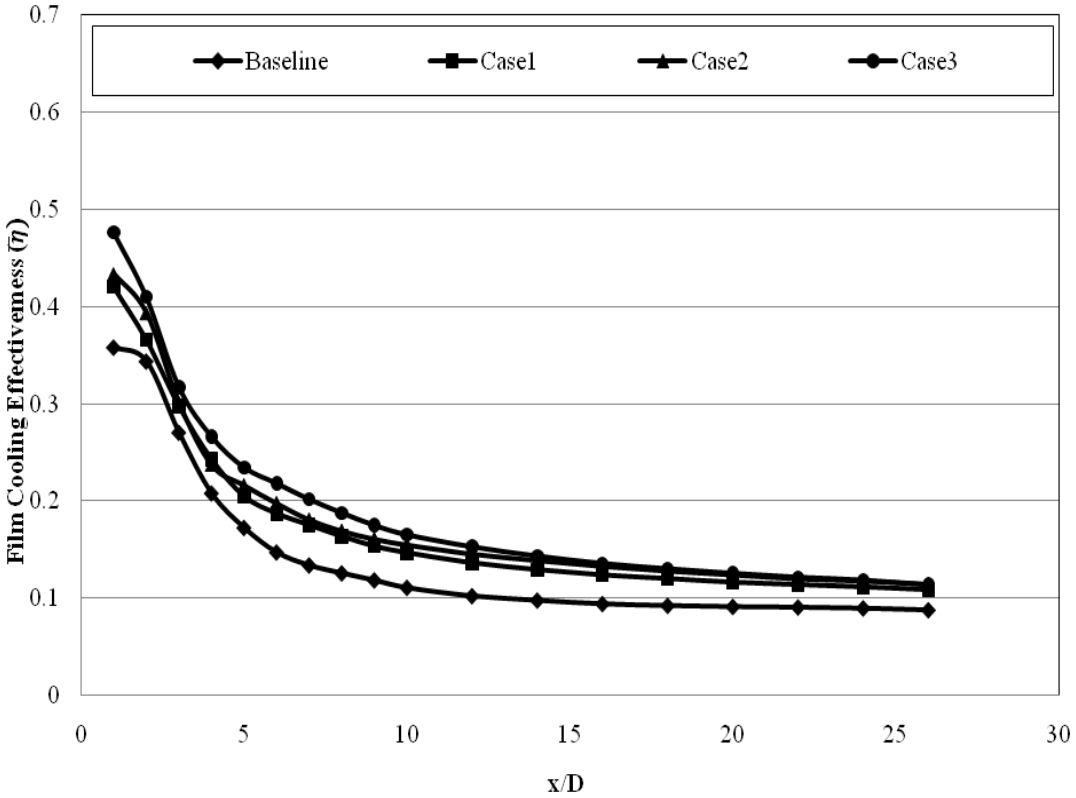


a) Under APG(2)

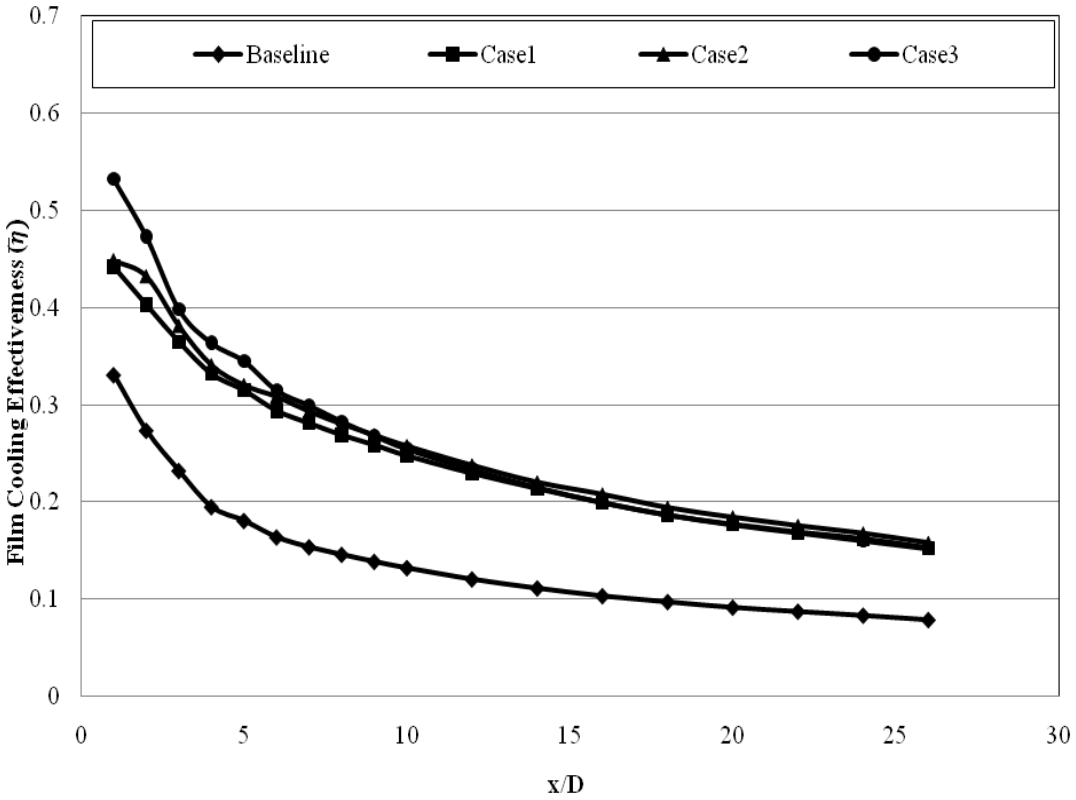


b) Under FPG

Figure (6.24) Spanwise Averaged Film Cooling Effectiveness Distribution under APG(2) and FPG at VR =0.5

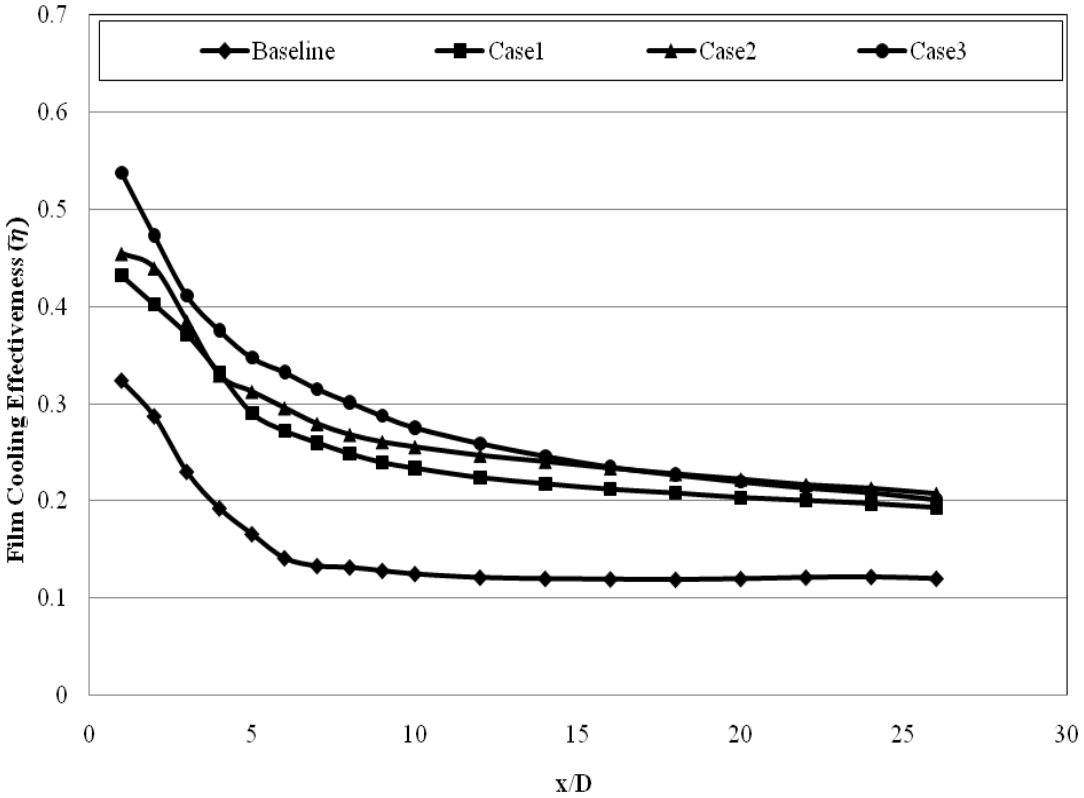


a) Under APG(2)

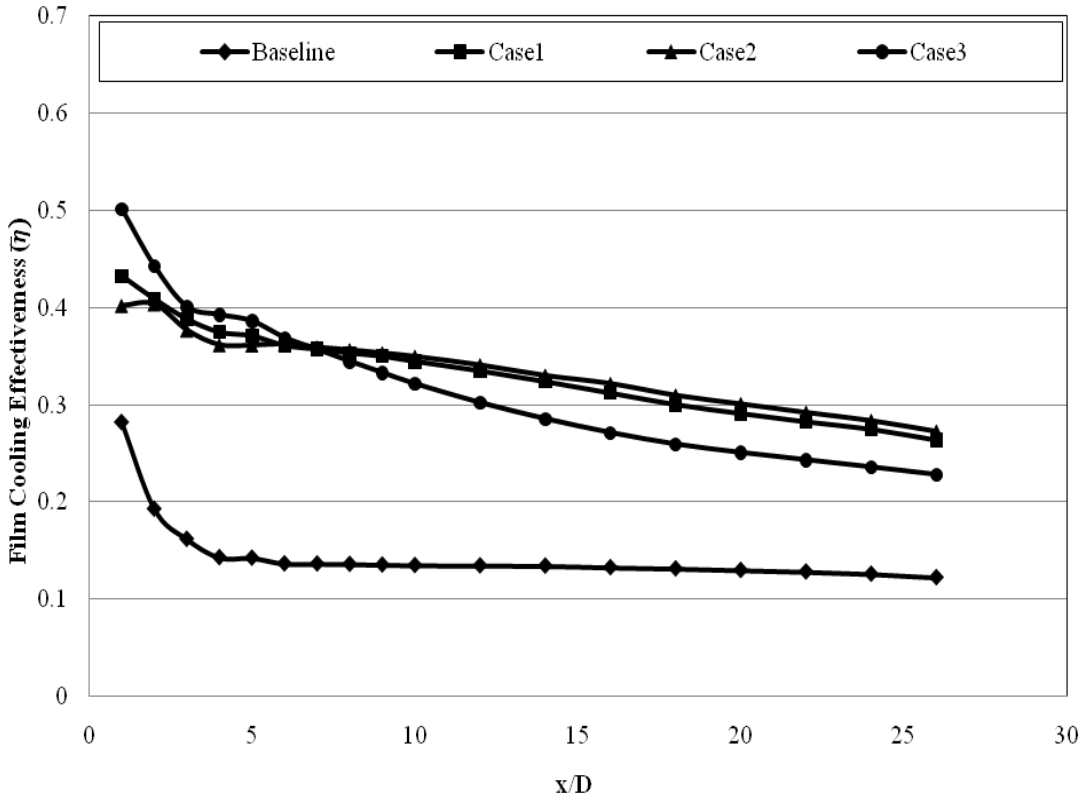


b) Under FPG

Figure (6.25) Spanwise Averaged Film Cooling Effectiveness Distribution under APG(2) and FPG at VR =1.0

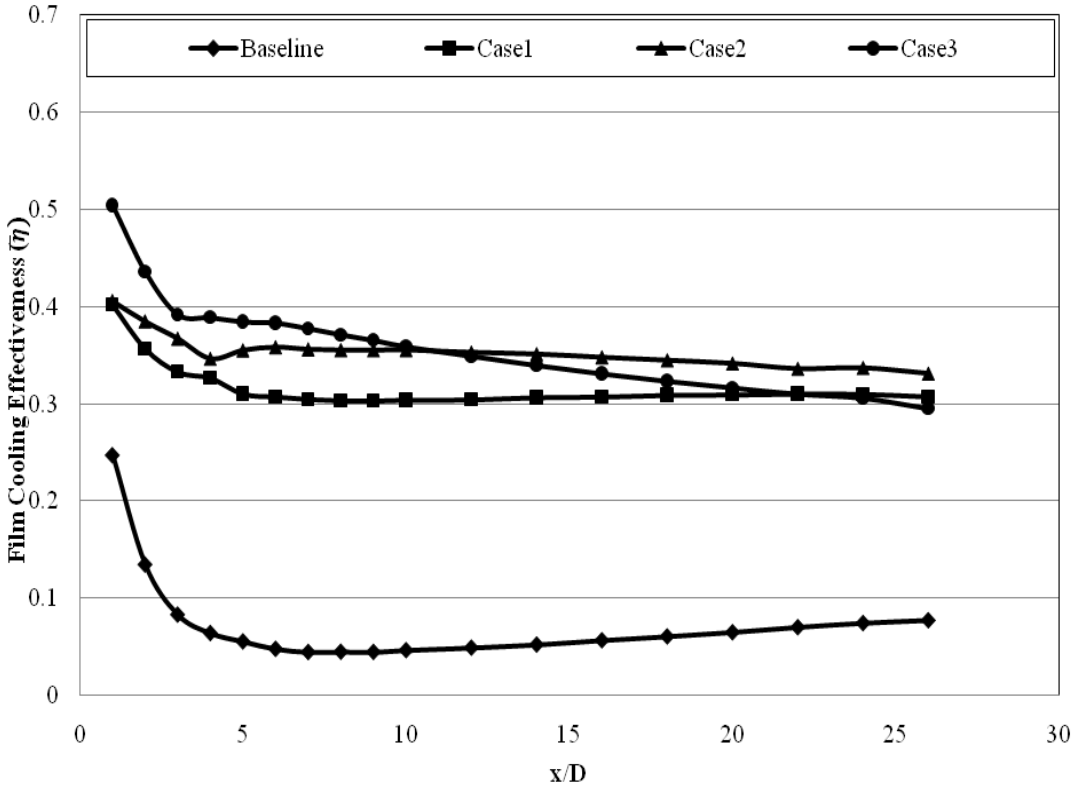


a) Under APG(2)

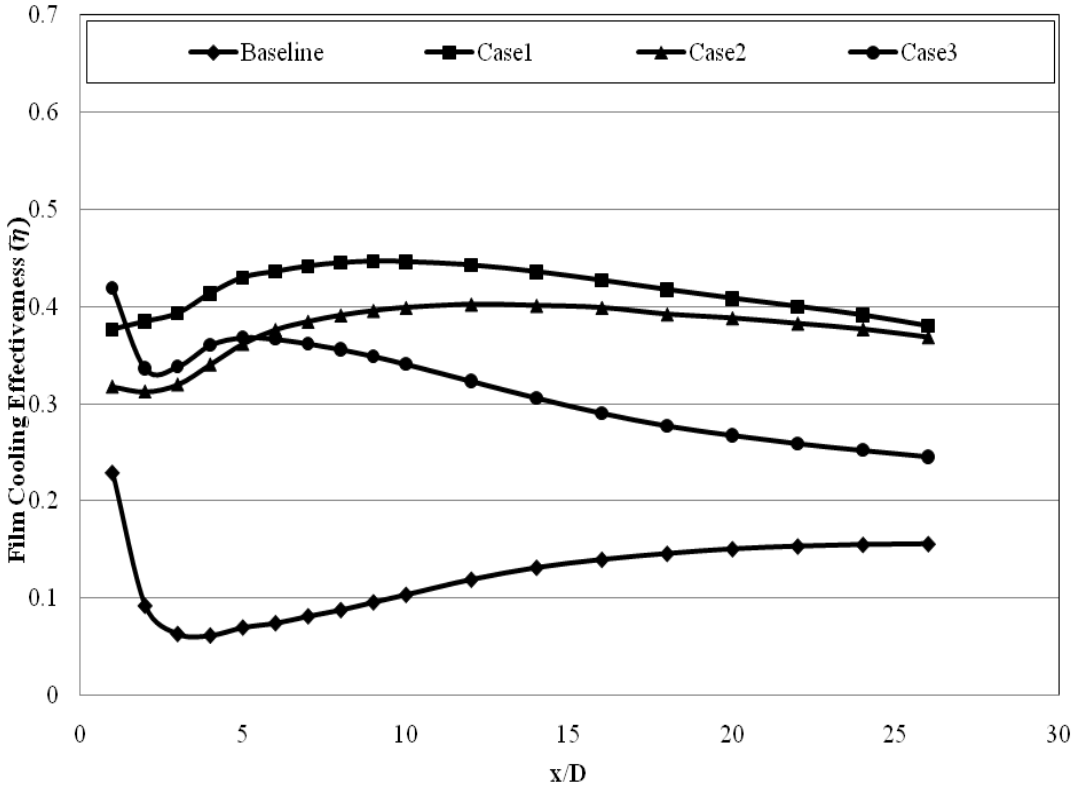


b) Under FPG

Figure (6.26) Spanwise Averaged Film Cooling Effectiveness Distribution under APG(2) and FPG at VR =2.0

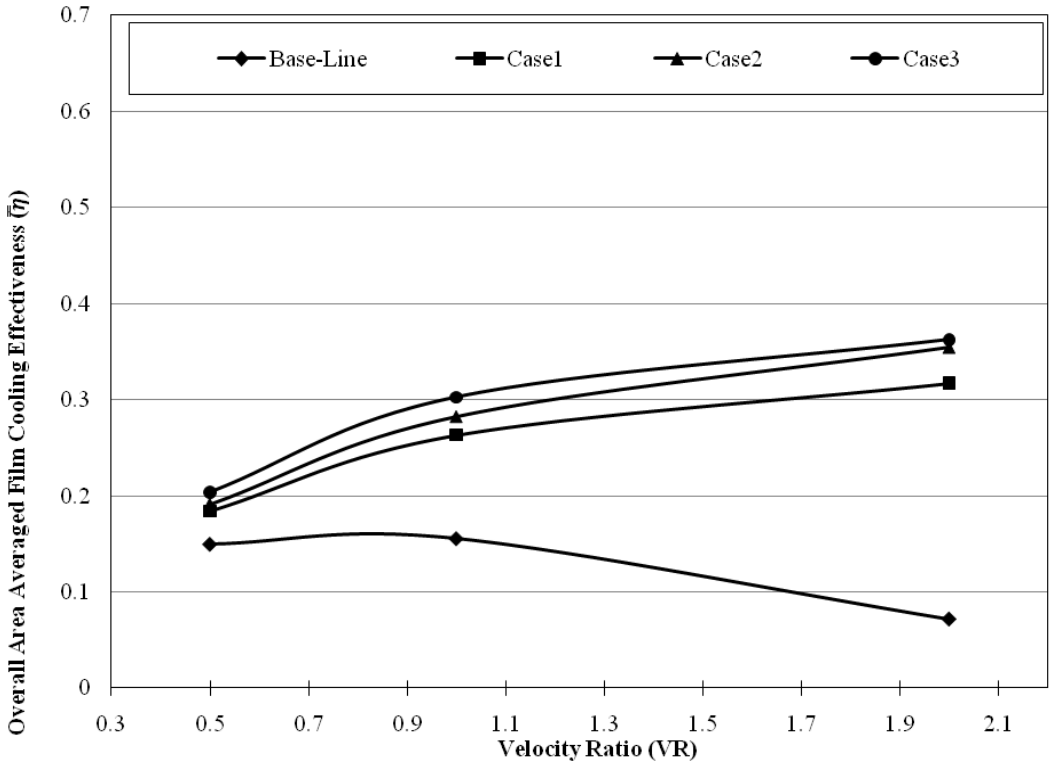


Figure (6.27) The overall area averaged film cooling effectiveness under APG(2) at different velocity ratios

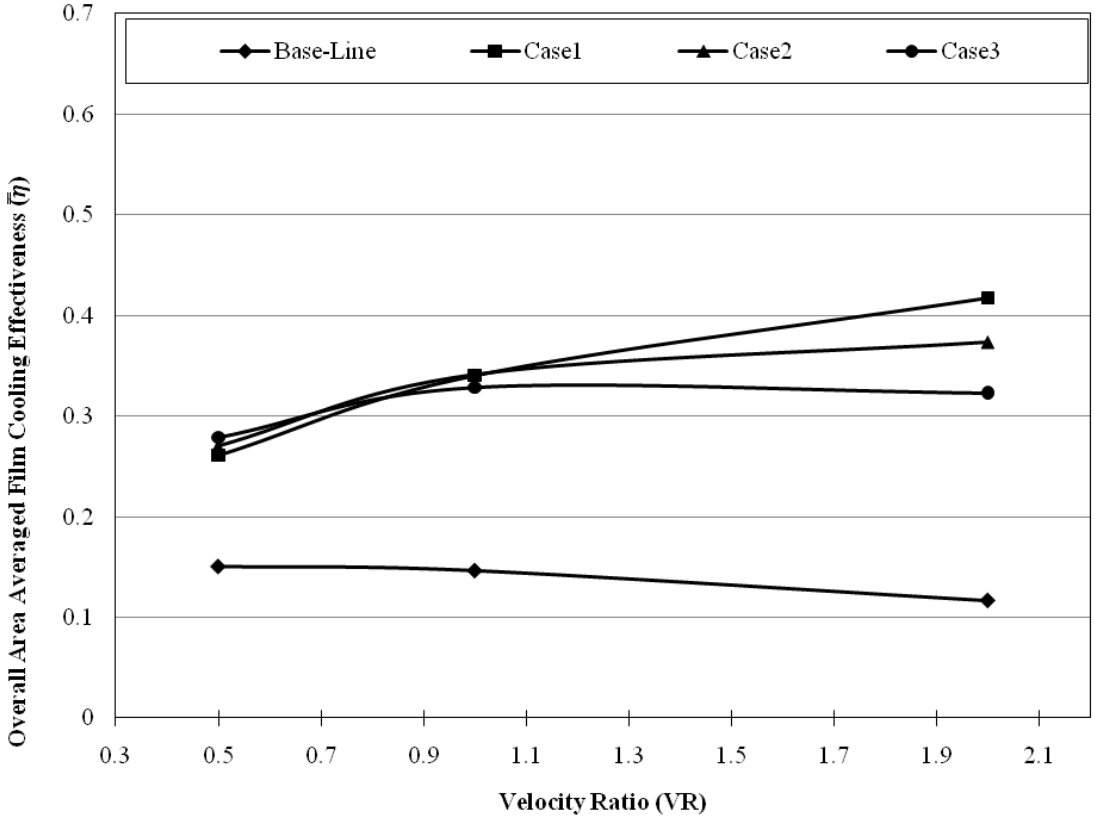


Figure (6.28) The overall area averaged film cooling effectiveness under FPG at different velocity ratios

### 6.4.3 Comparison between the Studied Pressure Gradients

Figures (6.29), (6.30), and (6.31) show the spanwise averaged film cooling effectiveness distribution for baseline under different pressure gradients at VR = 0.5, 1.0, and 2.0, respectively. At VR = 0.5, figure (6.29) shows that, both adverse and favorable pressure gradients reduce the film cooling effectiveness but with a slight difference as compared with ZPG. At VR = 1.0, figure (6.30) shows that, both adverse and favorable pressure gradients increase the film cooling effectiveness as compared with ZPG. At VR = 2.0, the film cooling effectiveness under adverse pressure gradient is very close to that under ZPG, while under favorable pressure gradient, it increases with a significant effect.

Figures (6.32), (6.33), and (6.34) show the spanwise averaged film cooling effectiveness distribution for case 1 under different pressure gradients at VR = 0.5, 1.0, and 2.0, respectively. The figures show that for all studied velocity ratios, the favorable pressure gradient increases the film cooling effectiveness while the adverse pressure gradient reduces the film cooling effectiveness. Further increase of the value of adverse pressure gradient shows higher reduction of film cooling effectiveness.

Figures (6.35), (6.36), and (6.37) show the spanwise averaged film cooling effectiveness distribution for case 2 under different pressure gradients at VR = 0.5, 1.0, and 2.0, respectively. The figures show the same conclusion as that given by case 1.

For Case 3, Figures (6.38), (6.39), and (6.40) show the spanwise averaged film cooling effectiveness distribution under different pressure gradients at VR = 0.5, 1.0, and 2.0, respectively. The favorable pressure gradient increases the film cooling effectiveness with a slight difference at VR = 0.5 and 1.0. While at VR = 2.0, FPG reduces the film cooling effectiveness. On the other hand, the adverse pressure gradient decreases the film cooling effectiveness at VR = 0.5 and VR = 1.0 and increases it at VR = 2.0 but all of these increase and reduction with a small difference which may be concluded that the pressure gradient has no considrable effect at high velocity ratio. For more understanding of the effecto pressure gradient, the boundary layer velocity distribution will be disscused in section 6.5.

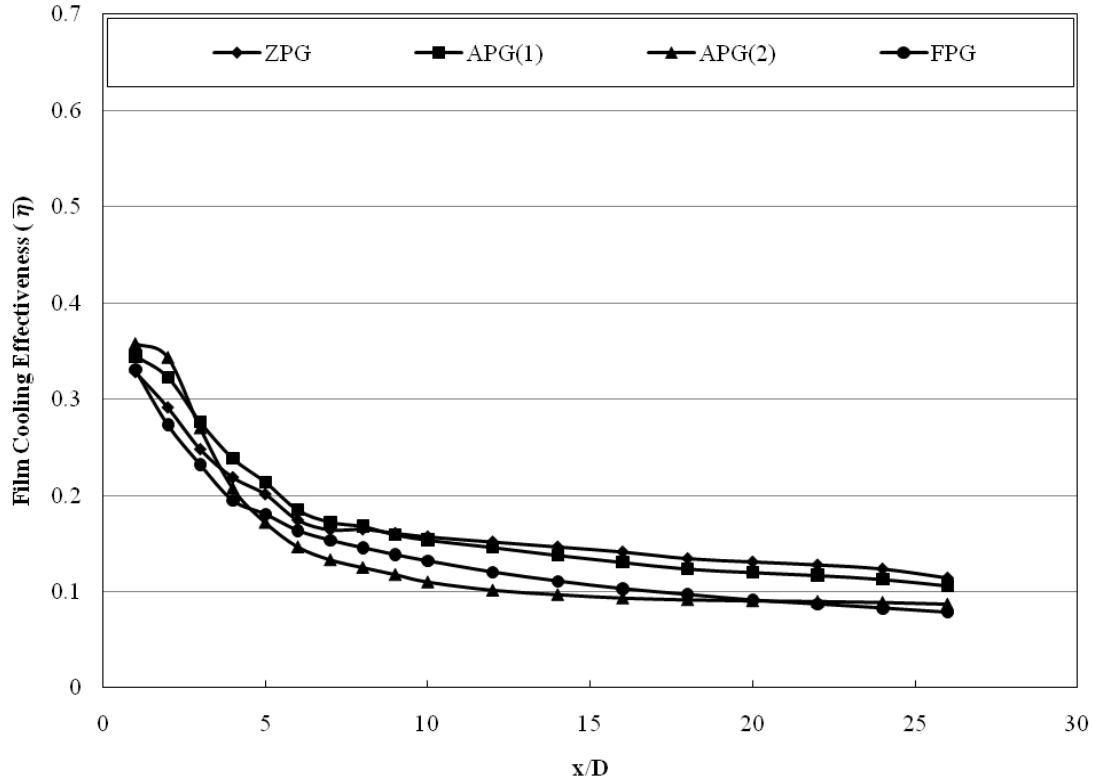


Figure (6.29) Spanwise Averaged Film Cooling Effectiveness Distribution for **baseline** under different pressure gradients at **VR = 0.5**

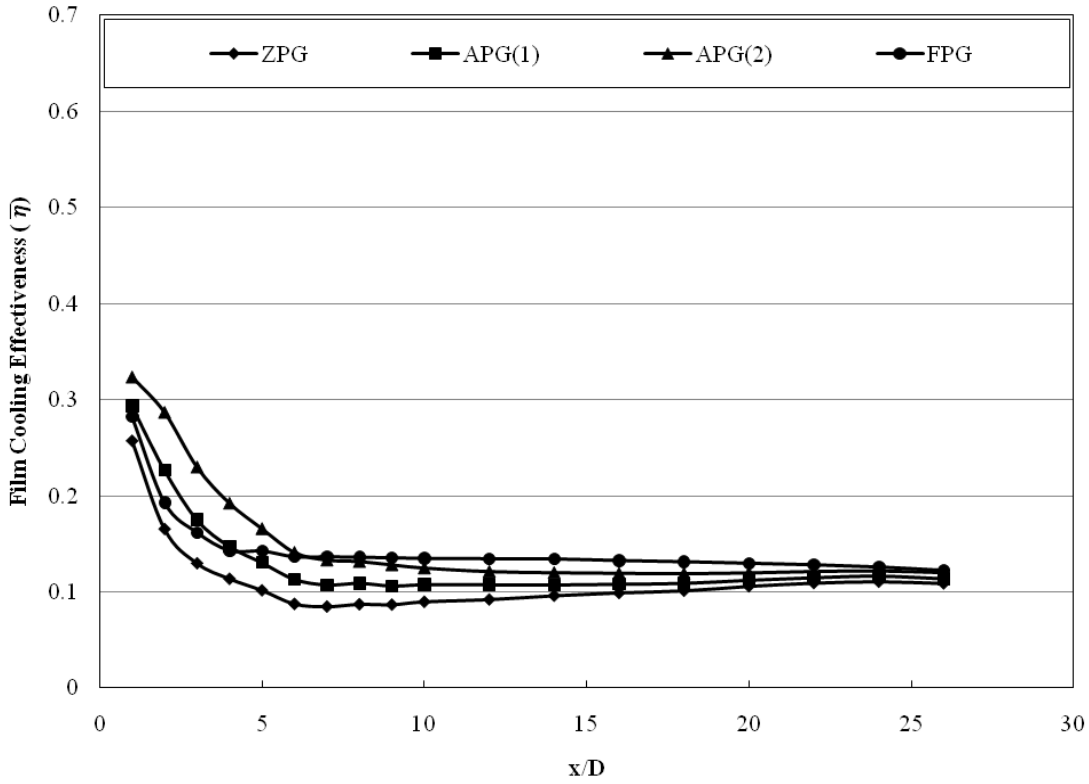


Figure (6.30) Spanwise Averaged Film Cooling Effectiveness Distribution for **baseline** under different pressure gradients at **VR = 1.0**

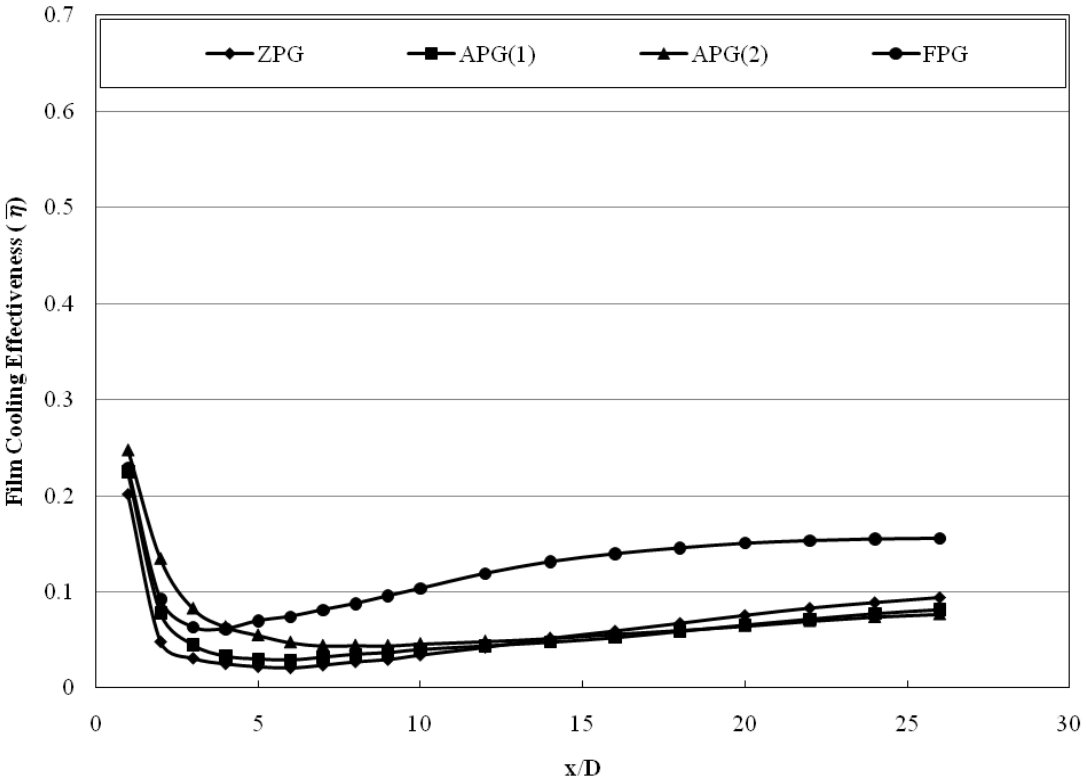


Figure (6.31) Spanwise Averaged Film Cooling Effectiveness Distribution for **baseline** under different pressure gradients at **VR = 2.0**

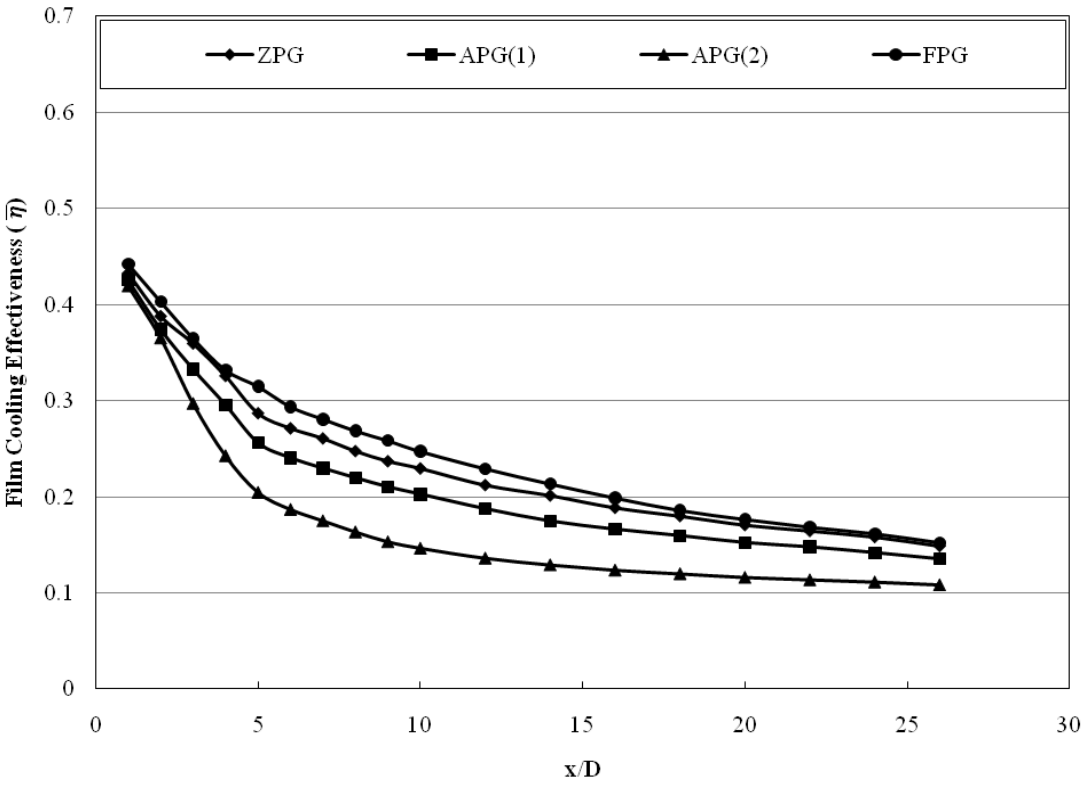


Figure (6.32) Spanwise Averaged Film Cooling Effectiveness Distribution for **Case 1** under different pressure gradients at **VR = 0.5**

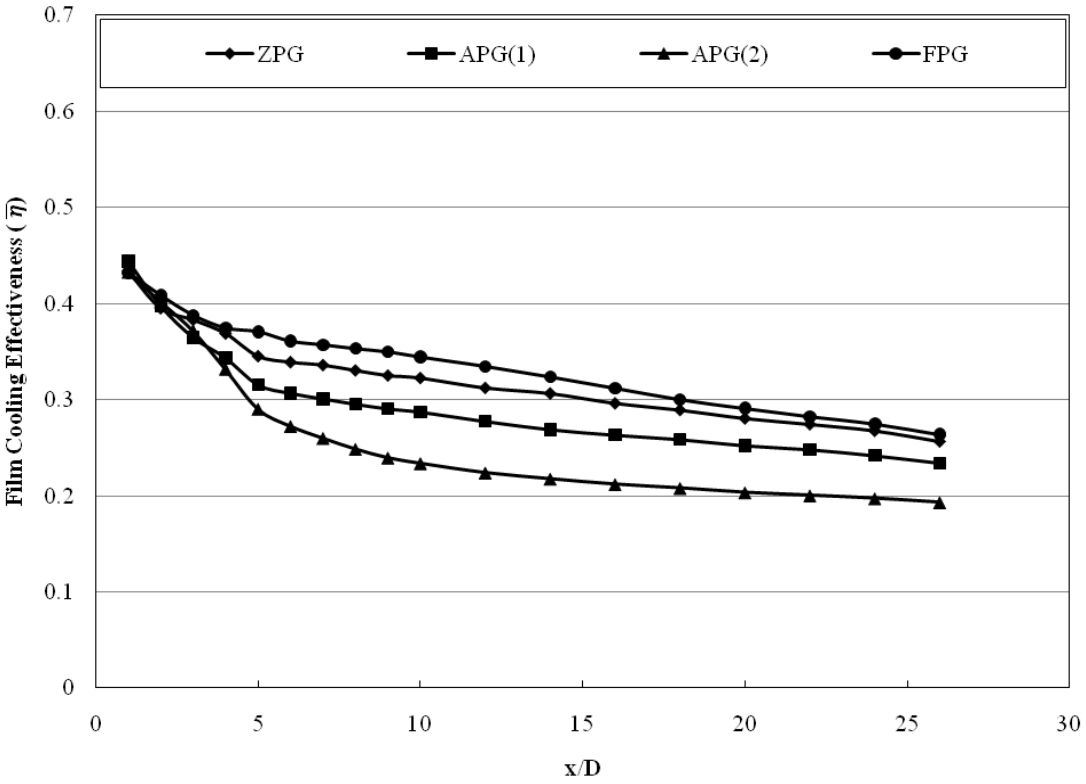


Figure (6.33) Spanwise Averaged Film Cooling Effectiveness Distribution for **Case 1** under different pressure gradients at **VR = 1.0**

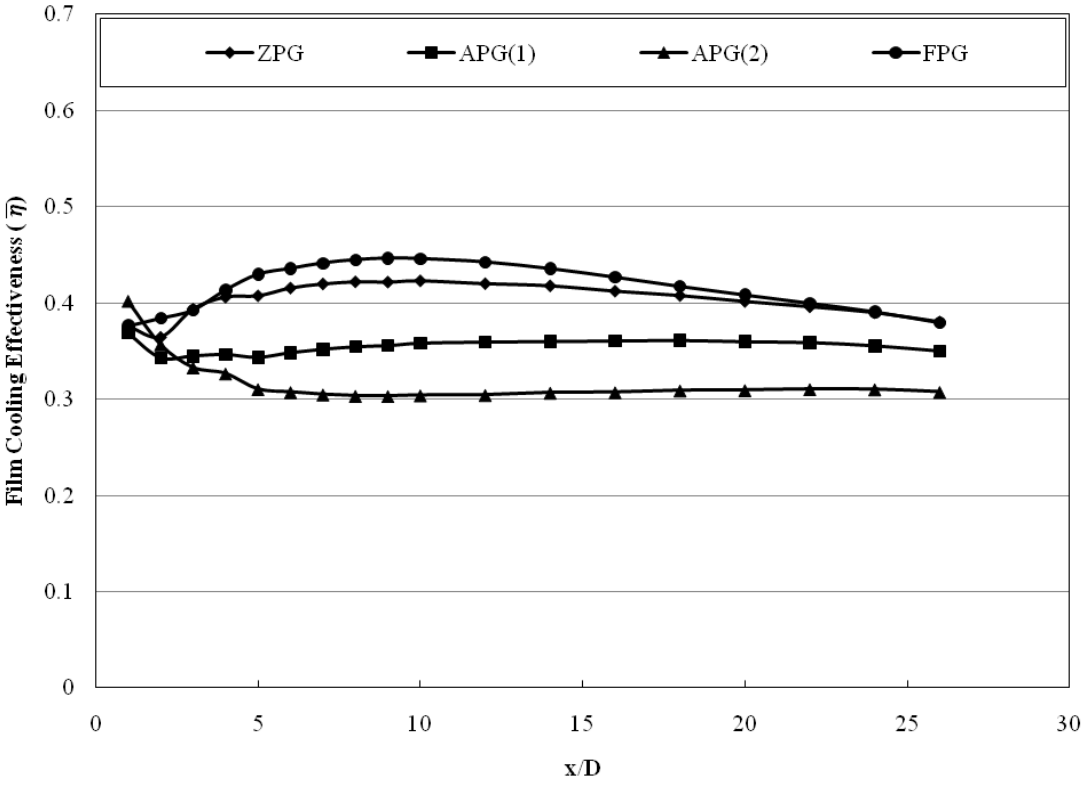


Figure (6.34) Spanwise Averaged Film Cooling Effectiveness Distribution for **Case 1** under different pressure gradients at **VR = 2.0**

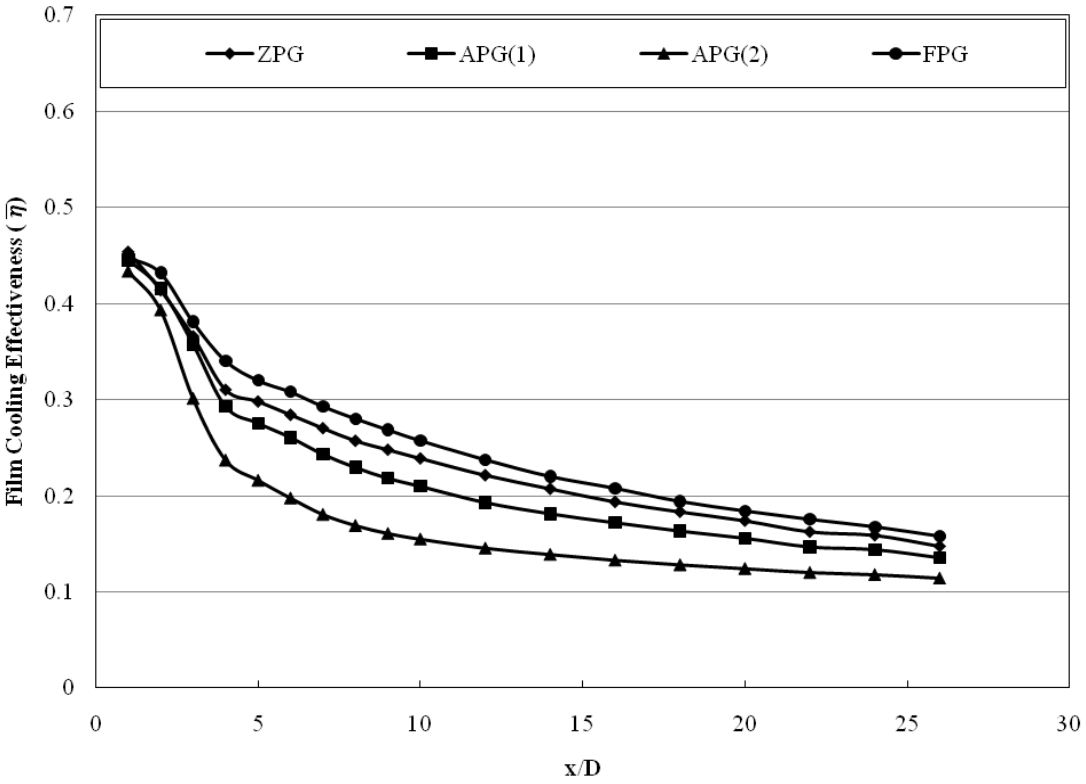


Figure (6.35) Spanwise Averaged Film Cooling Effectiveness Distribution for **Case 2** under different pressure gradients at **VR = 0.5**

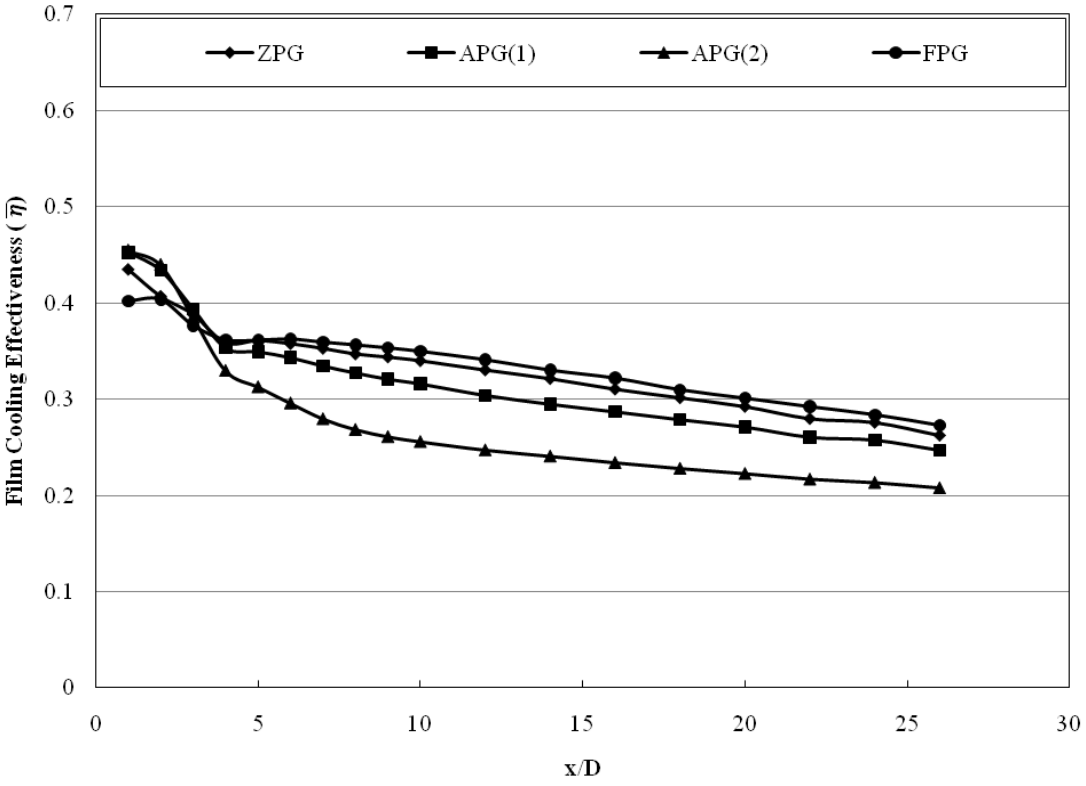


Figure (6.36) Spanwise Averaged Film Cooling Effectiveness Distribution for **Case 2** under different pressure gradients at **VR = 1.0**

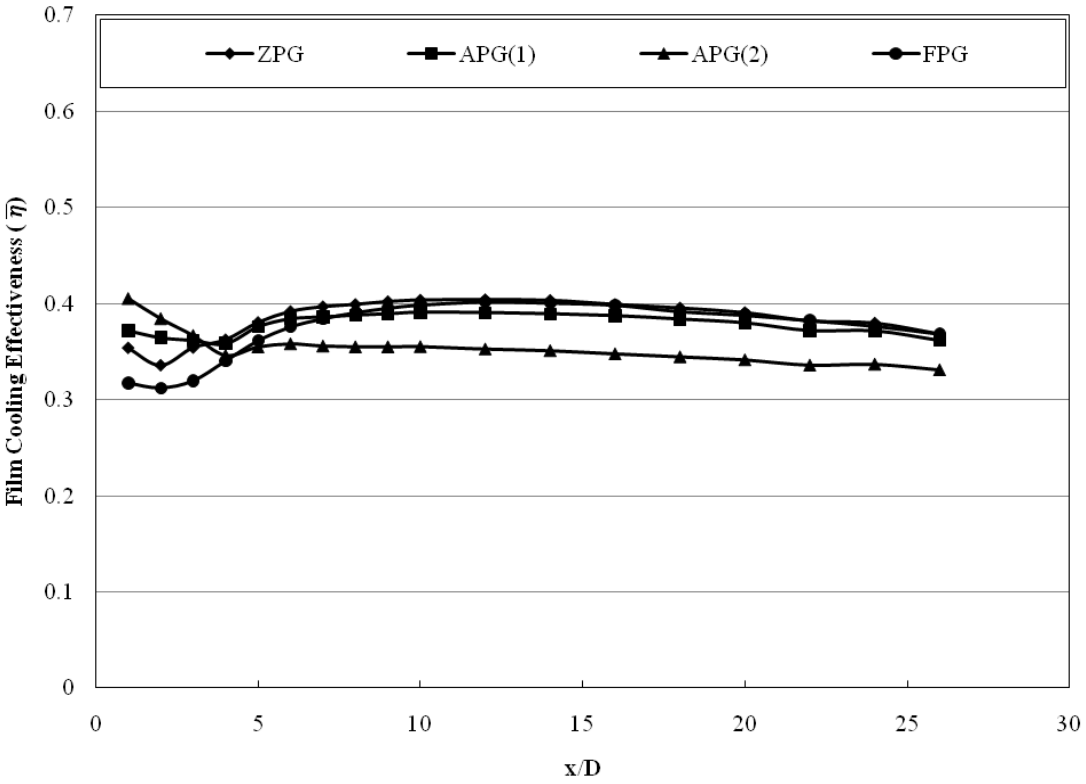


Figure (6.37) Spanwise Averaged Film Cooling Effectiveness Distribution for **Case 2** under different pressure gradients at **VR = 2.0**

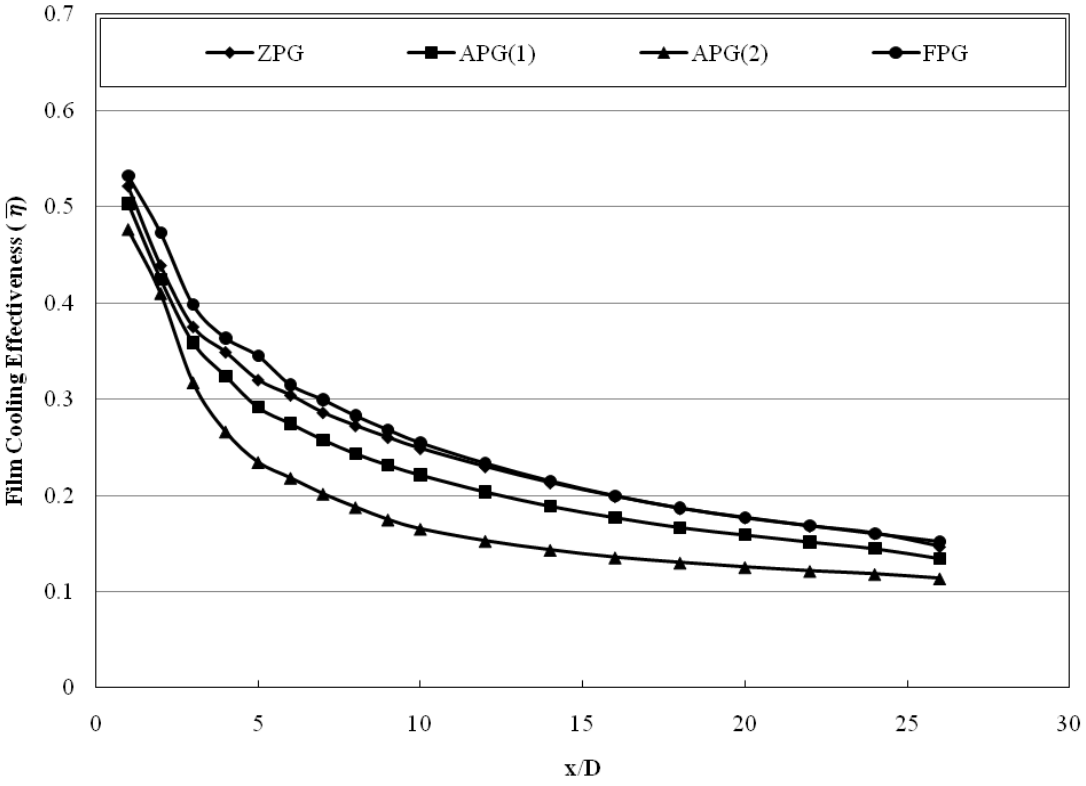


Figure (6.38) Spanwise Averaged Film Cooling Effectiveness Distribution for **Case 3** under different pressure gradients at **VR = 0.5**

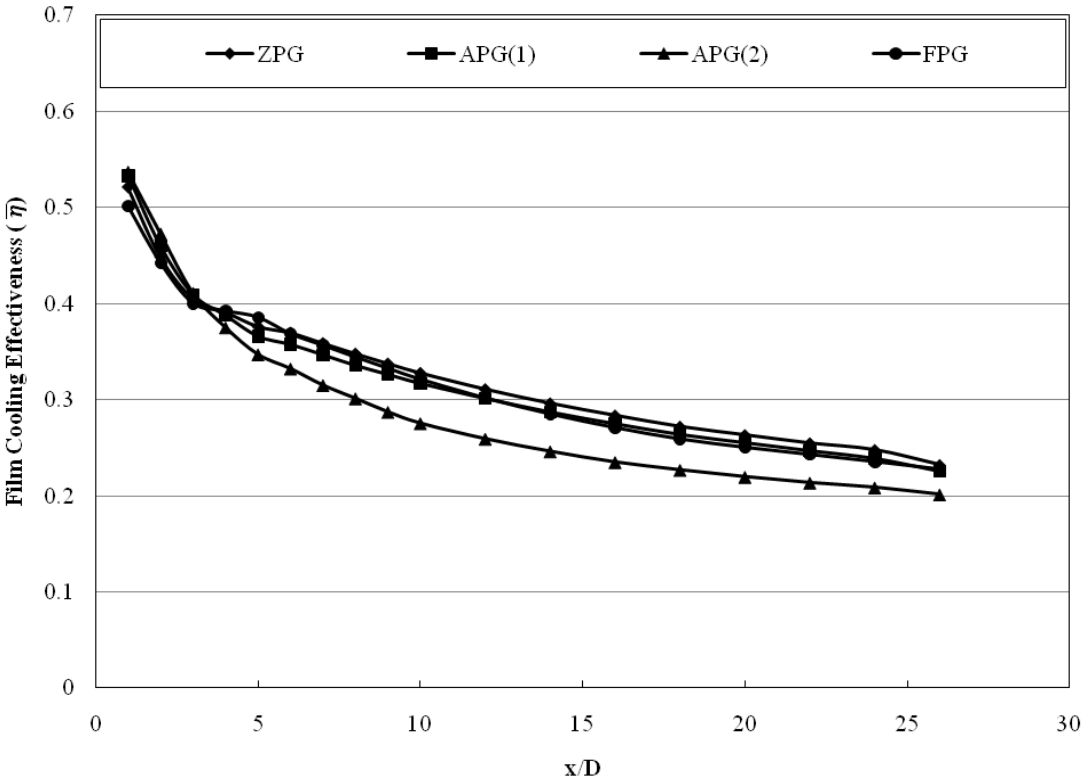


Figure (6.39) Spanwise Averaged Film Cooling Effectiveness Distribution for **Case 3** under different pressure gradients at **VR = 1.0**

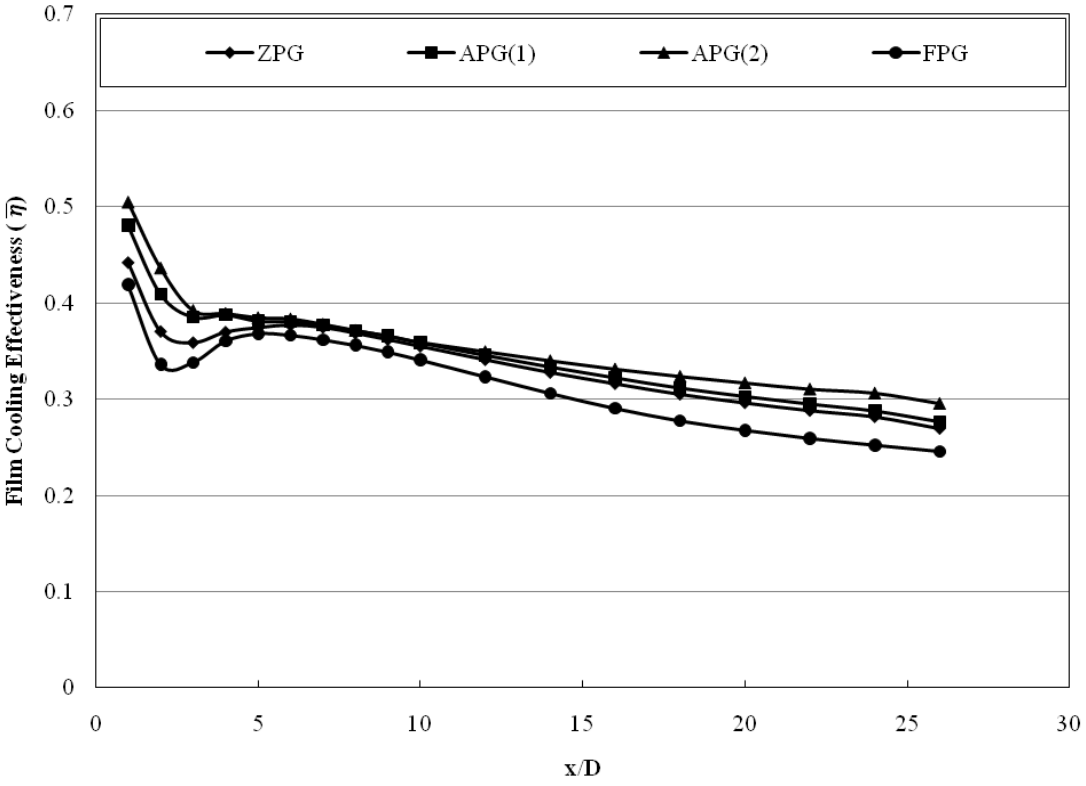


Figure (6.40) Spanwise Averaged Film Cooling Effectiveness Distribution for **Case 3** under different pressure gradients at **VR = 2.0**

## 6.5 Boundary Layer Velocity Distribution

According to the above results, the use of anti-vortex holes gives more enhancement in film cooling effectiveness than that is given by the traditional film cooling holes. That means the use of anti-vortex holes will gives more cooling for the turbine blades. To know how the anti-vortex holes work, the boundary layer velocity vectors will be discussed in the following paragraphs.

Figures (6.41), (6.42), (6.43), and (6.44) show a comparison between the boundary layer velocity distributions colored by effectiveness under ZPG, APG, and FPG for all cases at different values of velocity ratios. The boundary layer velocity distribution will be presented at x/D = 4 due to clear details of the interaction between the mainstream flow and the coolant jets.

For Baseline, Figure (6.41) shows two vortices due to the interaction between the mainstream flow and the jet flow. As the velocity ratio increases, the two vortices lift off the coolant jet away from the test surface due to high momentum flux. As the APG is applied, there is a suction area appearing near the top surface of the test section causing the free stream flow to move upward but due to the mass flux with respect to the cross-section area, the coolant jet still moves near the test surface. As the adverse pressure gradient increases, (APG(2)), the upward moving flow increases causing the coolant jet to lift off. Under FPG, the main flow has a velocity component moves towards the test surface and mitigate the coolant jet to move near the test surface.

For Case 1, figure (6.42) shows that there are new vortices, from the anti-vortex holes, appears above the two vortices coming out from the main hole. The new vortices try to move against the main hole vortices keeping the coolant flow near the test surface. This action is very clear with high velocity ratios but it is not clear with low velocity ratios because the fluid flow through the anti-vortex holes is taken from the main hole fluid and for low velocity ratios, the main hole flow is already low. When the adverse pressure is applied, the anti-vortex fluid flow is moving upward. Especially, the anti-vortex holes is upstream the main hole, that causes the coolant jet to move away from the test surface which reduces the film cooling effectiveness at the

test surface. But under the favorable pressure gradient the film cooling effectiveness increases due to the downward velocity component which keeps the coolant jets from the main hole and the anti-vortex holes near the test surface. Case 2 has the same performance like case 1 because the anti-vortex holes are still upstream the main hole. But, from figure (6.43) it is clearly that the flow from the anti-vortex holes is moving beside the flow from the main hole and creates new vortices against the main hole vortices but with covering a wider area than that covers in case 1.

For case 3, the fluid flow from the anti-vortex holes is moving below the fluid flow from the main hole because the anti-vortex holes are in line with the main hole and have a less momentum flux than the main hole. So, as shown in figure (6.44) the two vortices coming out from the main hole are lift off by the flow from the anti-vortex holes. When the pressure is applied the flow from the anti-vortex holes is still moving beside the test surface and saving by the main flow hole. So, there is no a significantly affect due to applied pressure gradient.

Figure (6.45) may be giving more understanding and good explanation for the film cooling distribution over the test surface. It shows the film cooling effectiveness distribution at test surface and x/D = 2, 8, and 15 for VR = 2 with ZPG.

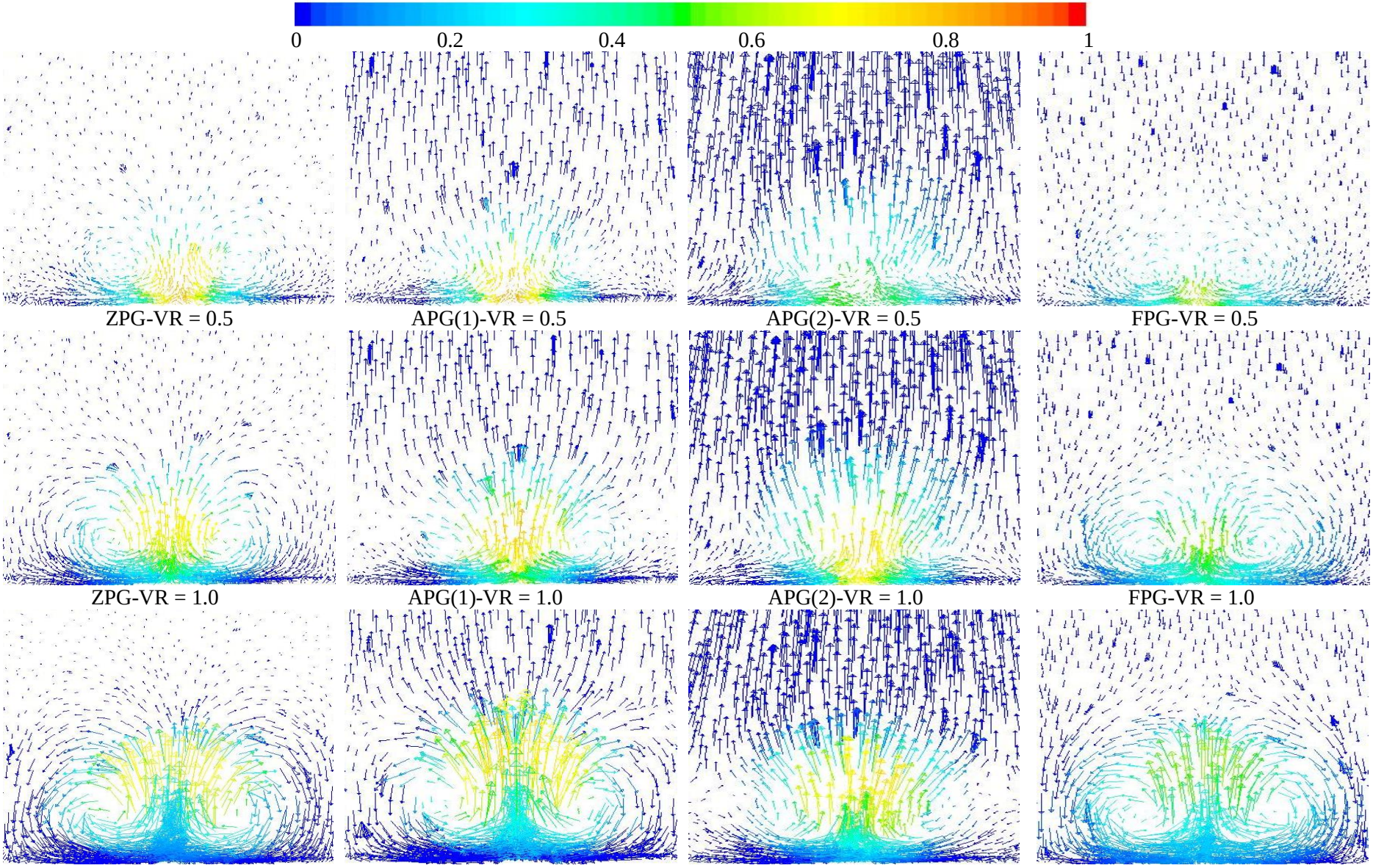


Figure (6.41) Secondary flow vectors colored by Effectiveness for Base line case under ZPG, APG, and FPG at different VR, x/D = 4

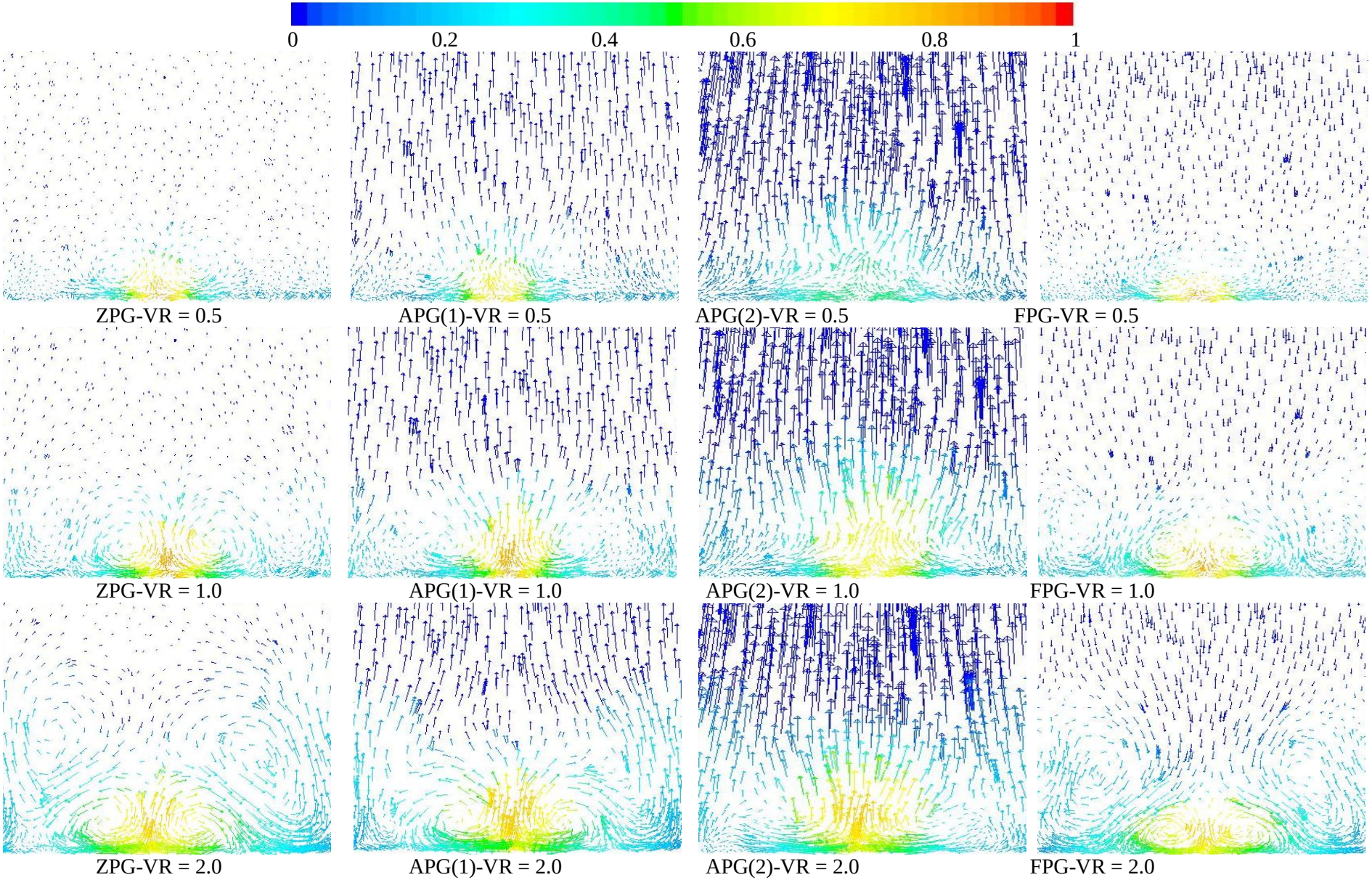


Figure (6.42) Secondary flow vectors colored by Effectiveness for Case-1 under ZPG, APG, and FPG at different VR, x/D = 4

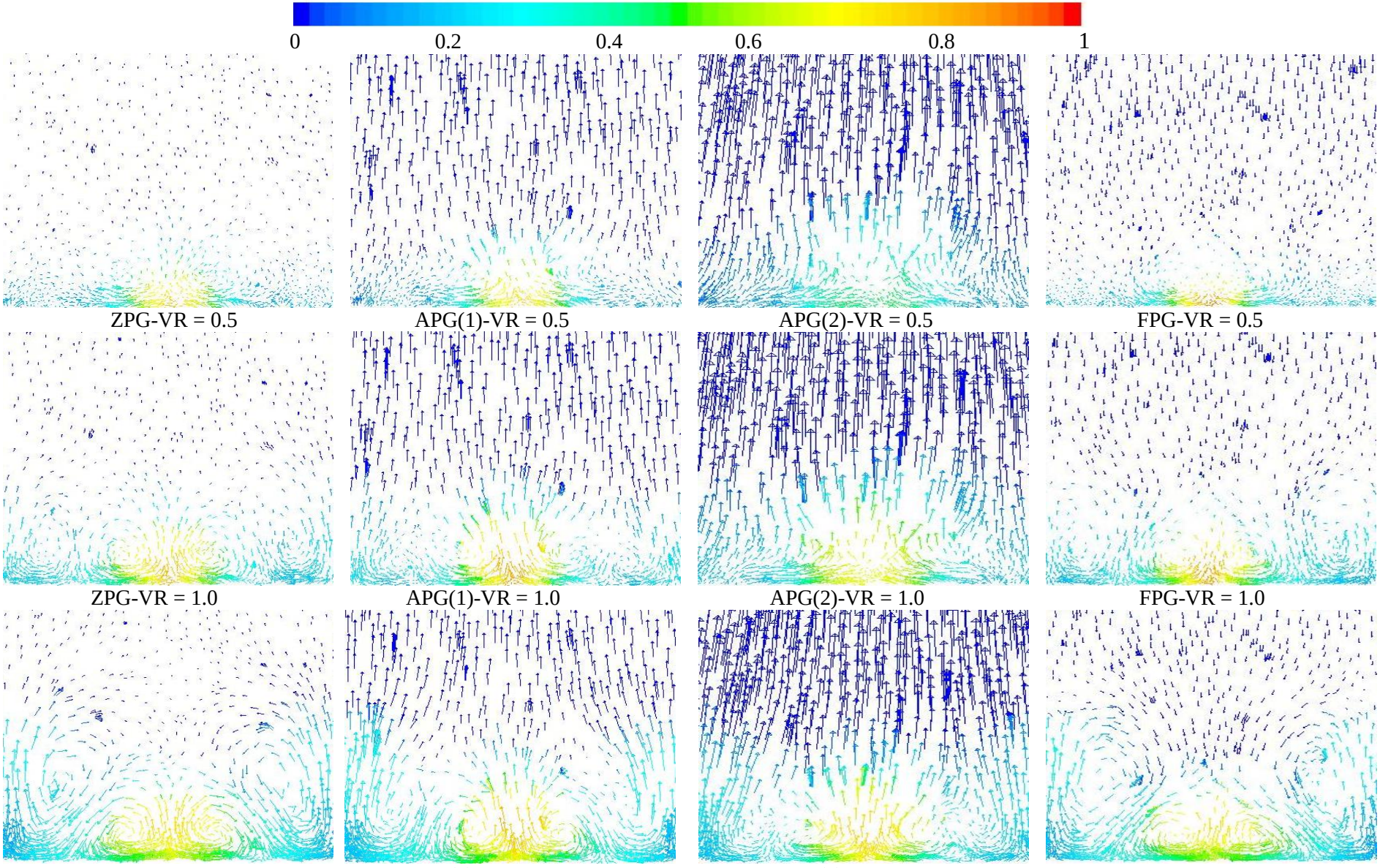


Figure (6.43) Secondary flow vectors colored by Effectiveness for Case-2 under ZPG, APG, and FPG at different VR, x/D = 4

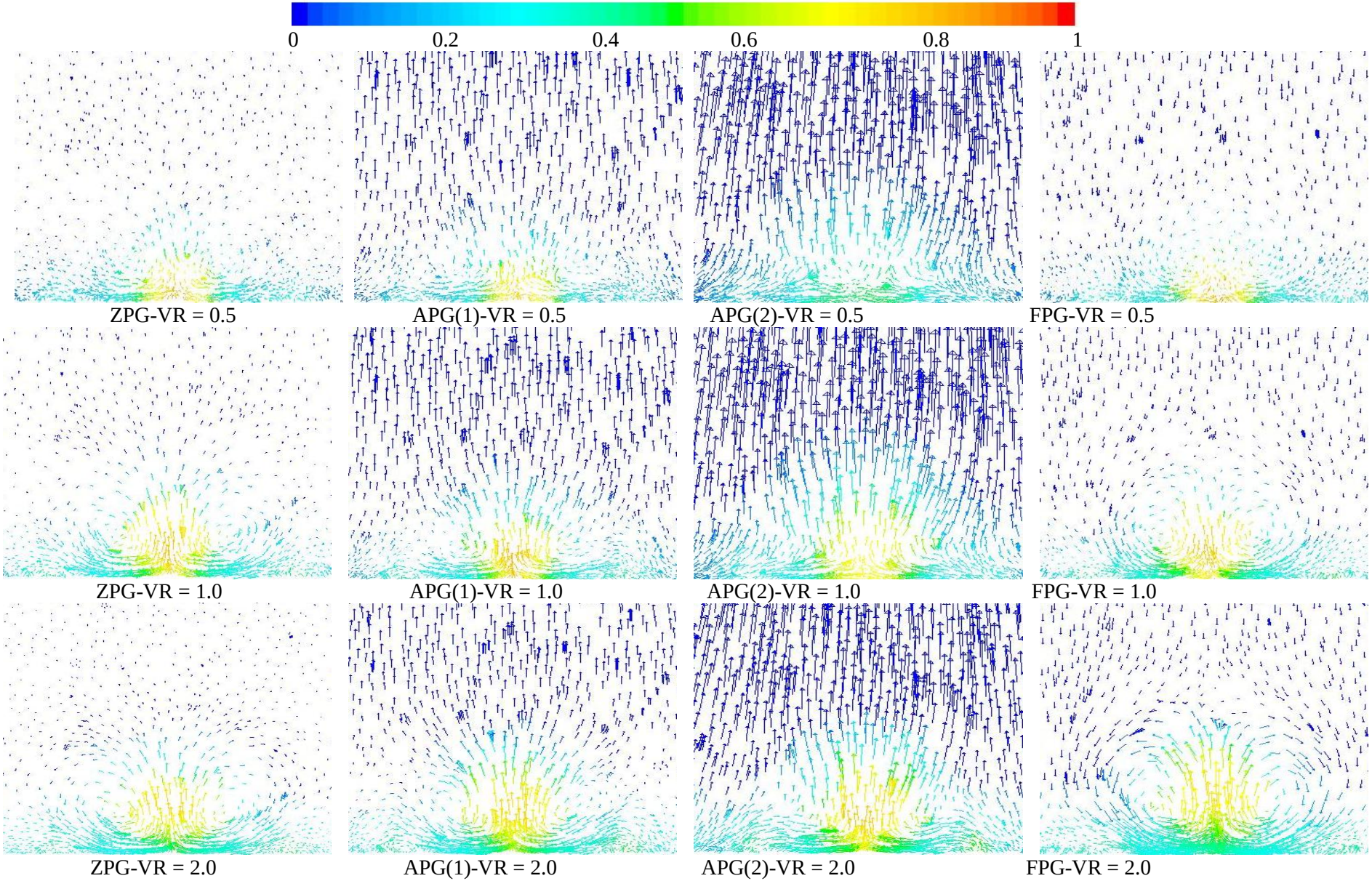


Figure (6.44) Secondary flow vectors colored by Effectiveness for Case-3 under ZPG, APG, and FPG at different VR, x/D = 4

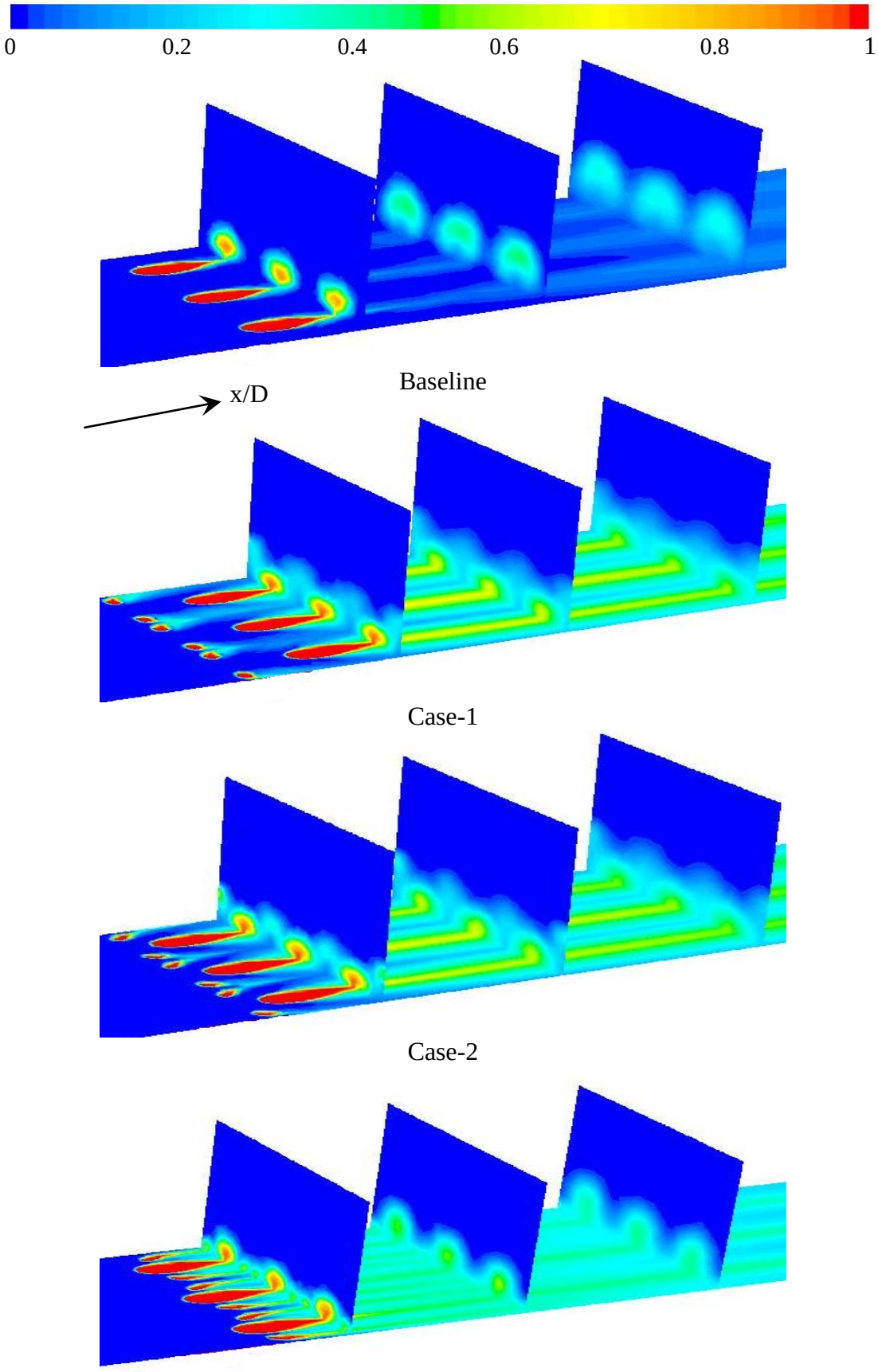


Figure (6.45) the detailed the film cooling effectiveness distribution at test surface and x/D = 2, 8, and 15 for VR = 2 under ZPG